

Uniaxial Compression and Indirect Tensile Testing of Cobourg Limestone: Influence of Scale, Saturation and Loading Rate

NWMO-TR-2017-17

December 2017

E. Jaczkowski, E. Ghazvinian and M. Diederichs

Department of Geological Science and Geological Engineering, Queen's University

nwmo

NUCLEAR WASTE
MANAGEMENT
ORGANIZATION

SOCIÉTÉ DE GESTION
DES DÉCHETS
NUCLÉAIRES



Nuclear Waste Management Organization
22 St. Clair Avenue East, 6th Floor
Toronto, Ontario
M4T 2S3
Canada

Tel: 416-934-9814
Web: www.nwmo.ca

Uniaxial Compression and Indirect Tensile Testing of Cobourg Limestone: Influence of Scale, Saturation and Loading Rate.

NWMO-TR-2017-17

December 2017

E. Jaczkowski, E. Ghazvinian and M. Diederichs
Department of Geological Science and Geological
Engineering, Queen's University

This report has been prepared under contract to NWMO. The report has been reviewed by NWMO, but the views and conclusions are those of the authors and do not necessarily represent those of the NWMO.

All copyright and intellectual property rights belong to NWMO.

Document History

Title:	Uniaxial Compression and Indirect Tensile Testing of Cobourg Limestone: Influence of Scale, Saturation and Loading Rate h		
Report Number:	TR-2017-17		
Revision:	R00	Date:	December 2017
Queen's University			
Authored by:	E. Jaczkowski, E. Ghazvinian and M. Diederichs Department of Geological Science and Geological Engineering, Queen's University		
Verified by:	Mark Diederichs		
Approved by:	Mark Diederichs		
Nuclear Waste Management Organization			
Reviewed by:	Tom Lam		
Accepted by:	Mark Jensen		

ABSTRACT

Title: Uniaxial Compression and Indirect Tensile Testing of Cobourg Limestone: Influence of Scale, Saturation and Loading Rate
Report No.: NWMO-TR-2017-17
Author(s): E. Jaczkowski, E. Ghazvinian and M. Diederichs
Company: Department of Geological Science and Geological Engineering, Queen's University
Date: December 2017

Abstract

An investigation of the stress-strain behaviour of Cobourg limestone has been conducted through the testing of 54 Uniaxial Compressive Strength (UCS) and 47 Brazilian Tensile Strength (BTS) specimens. The rock for these tests has been collected from St. Mary's Quarry located in Bowmanville, Ontario. At this site the unit is alternatively referred to as Cobourg or the Lindsay Formation.

This rock presents core scale heterogeneity in the form of large (50-75 mm) calcite rich nodules surrounded by more clay rich lenses. Specimens have been prepared with a length to diameter (L/D) ratio of 2.5 for UCS testing and a thickness to diameter (t/D) ratio of 0.5 for BTS testing. The influence of specimen water content and scale was studied for both UCS and BTS specimens, to investigate the elastic and strength properties of the rock. In addition, UCS specimens have been tested with varying axial strain rates to examine the effect of loading rate on the Cobourg limestone.

Oven drying as well as a number of saturation methods were used and compared in this study to investigate the efficiency of saturation and the impacts on the sample. The samples were saturated with synthetic formation pore water (SPW). Long term saturation by immersion (one to three months) is not efficient in increasing the level of saturation and, due to the unconfined nature of the sample while immersed, imparts non-realistic damage to the sample that is not representative of in situ saturation. Vacuum saturation did not prove markedly more effective than simple immersion over the same time frame (one week). One-week submersion effectively demonstrated the influence of resaturation and represents the most optimal resaturation time period for future investigations. However, due to the challenges of resaturating such low porosity rock, sample encapsulation after extraction is recommended for geomechanical testing.

For the purposes of comparison, 0.25% water content is taken as a datum corresponding to "Room Relative Humidity" (RRH). Average strength thresholds for three 76 mm diameter samples at 0.25% water content and standard loading rates for UCS, CD and CI are 107MPa, 85 MPa and 46 MPa respectively. Based on testing results, maximum achievable saturation was shown to decrease UCS by up to 14% compared to room relative humidity conditions (RRH) and Critical Damage (CD) by up to 15%. CI was reduced by a more modest 8%. Oven drying to 0.065% water content, on the other hand, increased the three thresholds by 24%, 26% and 13% respectively. BTS was reduced by up to 25% by saturation and increased by up to 20% by drying.

Scale effect was investigated through the testing of four different core specimen sizes (50, 76, 101 and 126 mm diameter). Young's modulus of the rock was seen to increase with increasing specimen diameter within the range of sizes tests. There has been no clear influence of scale on Poisson's ratio, CI, CD, or UCS of the Cobourg limestone. The BTS results have shown a decrease in strength with increasing specimen diameter with most of the decrease occurring between 50 and 76 mm.

The results of loading rate testing on Room Relative Humidity (RRH) and one-month saturated specimens have shown no significant effects to changing axial strain rate with respect to Young's modulus, Poisson's ratio, and CI threshold of the rock. The RRH specimen results show a moderate decrease in CD and UCS threshold with increasing axial strain rate, while one-month saturated specimens the opposite trend.

Table of Contents

	<u>Page</u>
ABSTRACT	iii
LIST OF TABLES	vii
Page	vii
1. Introduction	1
2. Work Scope.....	1
3. Testing Plan	1
4. Specimen Preparation	6
4.1 Sample Collection	6
4.2 Drilling, Cutting, Grinding.....	7
4.3 Verification of Dimensions	9
4.3.1 UCS Specimens	9
4.3.2 BTS Specimens.....	11
4.4 Photography and Scanning.....	11
4.4.1 Blocks	11
4.4.2 Cores.....	11
4.4.3 Specimens.....	12
4.4.4 Test Setup	14
4.5 Saturation and Drying Methods	14
4.6 Water Content and Bulk Density Measurements.....	16
5. Testing Configuration and Procedures	17
5.1 Equipment.....	17
5.1.1 MTS 815 Rock Mechanics Testing System	17
5.1.2 Acoustic Emission (AE) Monitoring System	18
5.1.3 Strain Gauges	19
5.2 UCS Testing Procedure.....	19
5.2.1 Axial and Circumferential Deformation Rates.....	20
5.3 BTS Testing Procedure.....	21
6. Data Processing Methodology.....	24
6.1 Water Content.....	24
6.2 Bulk Density.....	24
6.3 Elastic Parameters	24
6.4 Uniaxial Compressive Strength (UCS)	25
6.5 Brazilian Tensile Strength (BTS).....	25
6.6 Crack Initiation (CI) and Crack Damage (CD) Estimation	25
6.6.1 Direct Strain [CI/CD]	25
6.6.2 Crack Volumetric Strain [ϵ_{cv}]	26
6.6.3 Inverse Tangent Lateral Stiffness (ITLS)	27
6.6.4 Instantaneous Poisson's Ratio [$\nu\Delta$].....	27
6.6.5 Instantaneous Young's Modulus [CD].....	27
6.6.6 Acoustic Emission (AE) Methods [CI/CD].....	28
7. Results	29
7.1 Uniaxial Compressive Strength (UCS) Results	29
7.1.1 Saturation	29

7.1.2	Scale	34
7.1.3	Loading Rate	37
7.1.4	Room Relative Humidity (RRH) Results.....	38
7.2	Brazilian Tensile Strength (BTS) Results	44
7.2.1	Saturation	44
7.2.2	Scale	46
8.	Conclusion	47
References	49

LIST OF TABLES

	Page
Table 1: List of UCS specimens used to examine the effect of saturation.	2
Table 2: List of BTS specimens used to examine the effect of saturation.	3
Table 3: List of UCS specimens used to examine the effect of scale.	4
Table 4: List of BTS specimens used to examine the effect of scale.	4
Table 5: List of UCS specimens used to examine the effect of loading rate.	5
Table 6: Axial and circumferential deformation rates used for each test type.	20
Table 8: Summary of water content results.	30
Table 9: Young's modulus (E35) and Poisson's Ratio (ν 35) data for saturation specimens.	31
Table 10: Thresholds from Best Fit Trends for dried, RRH, and saturated specimens.	32
Table 11: UCS and crack damage threshold data for saturation specimens.	33
Table 12: Young's modulus (E35) and Poisson's ratio (ν 35) for scale specimens.	35
Table 13: UCS and crack damage threshold data for scale specimens.	36
Table 14: Summary of deformation and strain rates used to achieve targeted failure times.	38
Table 15: Young's modulus (E35) and Poisson's ratio (ν 35) data for RRH loading rate specimens.	39
Table 16: UCS and crack damage threshold data for RRH loading rate specimens.	40
Table 17: Young's modulus (E35) and Poisson's ratio (ν 35) data for one-month saturated loading rate specimens.	42
Table 18: UCS and crack damage threshold data for one-month saturated loading rate specimens.	43
Table 19: BTS data for saturation specimens.	45
Table 20: BTS data for scale specimens.	46

LIST OF FIGURES

Figure 1: Saint Mary's Quarry. Sample location shown by black arrow.	6
Figure 2: Water-cooled cutting of Cobourg blocks using a flexible chain saw at Pierrexpert, Montreal.	7
Figure 3: (a) Marking the drilling location and size on top of the Cobourg limestone blocks, (b) securing the block at the base of the drilling machine, (c) drilling a Cobourg limestone block.	8
Figure 4: (a) Diamond saw for cutting cores, (b) Specimen grinder with diamond grinding cup-wheel.	8
Figure 5: Granite support surface, digital indicator, V-block, feeler gage, and the electronic caliper used for verification of the specimen dimensions.	9
Figure 6: Verification of the flatness and parallelism of the specimen ends.	10
Figure 7: Drilled cores are photographed in dry and wet (surface) conditions.	12
Figure 8: (a) One of the four sides of prepared specimens are photographed at 90° radial increments before testing, (b) an example for an unrolled image of a Cobourg limestone circumferential surface produced by the cylinder scanner.	12
Figure 9: Photograph of the bottom of two prepared BTS specimens.	13
Figure 10: Cylinder scanner used for capturing the unrolled circumferential surface of the specimens.	13
Figure 11: Apparatus used for vacuum saturation of the specimens.	14
Figure 12: Stainless steel trays used during vacuum saturation.	15
Figure 13: VWR oven used to dry UCS and BTS specimens.	16
Figure 14: MTS rock mechanics testing system at the Queen's Geomechanics testing laboratory.	17
Figure 15: PAC Pocket AE monitoring system, PAC R15 sensors, and accessories.	18
Figure 16: UCS test set-up for Cobourg limestone specimens.	21
Figure 17: BTS test set-up for 50 and 76 mm Cobourg limestone specimens.	22
Figure 18: BTS test set-up for 101 and 126 mm Cobourg limestone specimens.	23
Figure 19: Example of strain-stress graph showing axial, lateral, and volumetric strain data and their associated CI and CD threshold markers.	26
Figure 20: Comparison of water content and saturation method for UCS specimens.	30
Figure 21: Poisson's ratio and Young's modulus (GPa) compared to the water content.	31
Figure 22: Comparison of CI, CD, and UCS stress thresholds with respect to specimen water content.	32
Figure 23: Crack Initiation (CI) indicator for saturation specimens based on six different methods: direct lateral strain, crack volumetric strain, inverse tangent lateral stiffness, instantaneous Poisson's ratio, acoustic emissions, and mean values from all methods.	34
Figure 24: Poisson's ratio and Young's modulus compared to specimen diameter.	35
Figure 25: Comparison of CI, CD, and UCS stress thresholds with respect to specimen diameter.	36
Figure 26: Crack Initiation (CI) indicator for scale specimens based on six different methods: direct lateral strain, crack volumetric strain, inverse tangent lateral stiffness, instantaneous Poisson's ratio, acoustic emissions, and mean values from all methods.	37
Figure 27: Poisson's ratio and Young's modulus vs axial strain rate for RRH. The blue arrow represents the standard axial strain rate used for saturation and scale tests.	38

Figure 28: Comparison of CI, CD, and UCS stress thresholds with respect to axial strain rate for RRH specimens. The blue arrow represents the standard axial strain rate used for saturation and scale tests.	39
Figure 29: Crack Initiation (CI) indicator for RRH specimens based on six different methods: direct lateral strain, crack volumetric strain, inverse tangent lateral stiffness, instantaneous Poisson's ratio, acoustic emissions, and mean values from all methods. The blue arrow represents the standard axial strain rate.	40
Figure 30: Poisson's ratio and Young's modulus compared to the axial strain rate for one-month saturated specimens. The blue arrow represents the standard axial strain rate used for saturation and scale tests.	41
Figure 31: Comparison of CI, CD, and UCS stress thresholds with respect to axial strain rate for one-month saturated specimens. The blue arrow represents the standard axial strain rate used for saturation and scale tests.	42
Figure 32: Crack Initiation (CI) indicator for one-month saturated specimens based on six different methods: direct lateral strain, crack volumetric strain, inverse tangent lateral stiffness, instantaneous Poisson's ratio, acoustic emissions, and mean values from all methods. The blue arrow represents the standard axial strain rate used for saturation and scale tests.	43
Figure 33: Comparison of water content and saturation method for BTS specimens.....	44
Figure 34: Comparison of BTS with respect to water content for saturation specimens.....	45
Figure 35: Comparison of BTS with respect to specimen diameter for scale specimens.	46

1. INTRODUCTION

The excavation damaged zone (EDZ) research project at the Queen's University Geomechanics Group includes laboratory investigation of Cobourg limestone mechanical properties. This project is aimed at establishing a reliable protocol for future laboratory testing of Cobourg limestone or alike material. The specimens in this test series have been prepared from large blocks of Cobourg limestone, retrieved from St. Mary's Quarry near Bowmanville, Ontario.

Uniaxial Compressive Strength (UCS) testing has been conducted on a total of 54 specimens to address the influence of saturation, loading rate, scale, and the combinations of these parameters on the measured geomechanical properties of the Cobourg limestone. The influence of saturation and scale has been further investigated through Brazilian Tensile Strength (BTS) testing of 47 specimens. The purpose of this report is to present the result of this testing, summarize the effect of saturation, loading rate, and scale on the geomechanical properties of Cobourg limestone, and discuss the effectiveness of the testing program with respect to characterization of the rock.

2. WORK SCOPE

This testing program has been conducted in order to examine the influences of various testing conditions on the geomechanical properties of Cobourg limestone. This report will discuss the methodology used to collect, prepare, and test Uniaxial Compressive Strength (UCS) and Brazilian Tensile Strength (BTS) specimens. This will include the retrieval of samples, the drilling, cutting, and grinding of specimens, specimen testing condition preparation, and the procedures and equipment used during testing. In addition, methods used to calculate properties such as water content, bulk density, Crack Initiation (CI) threshold, Critical Damage (CD) threshold, UCS, and BTS will also be outlined. The results of testing will be presented and discussed with respect to specimen condition and ability to accurately characterize the geomechanical properties of Cobourg limestone. The quality assurance and quality control (QA/QC) of this testing will also be discussed, with reference to the Queen's Geomechanics Research Quality Plan (QU0001-01) and in accordance with the APM Design and Technical Project Quality Plan (APM-PLAN-01913-0222-R000).

3. TESTING PLAN

For this test program, three variations in specimen testing conditions were investigated: varying the saturation level of specimens (saturation effect), the size of the specimens (scale effect), and the time to failure of the specimens (loading rate effect). The effect of saturation was investigated through 18 Uniaxial Compressive Strength (UCS) and 30 Brazilian Tensile Strength (BTS) tests. The UCS specimens used in this testing had a diameter of 76 mm and a consistent length to diameter ratio (L/D) of 2.5. The loading rate was set to achieve failure in approximately 20 minutes. To better control the near yield and post yield behaviour, an axial displacement control rate, for the 76mm diameter samples, of 0.01mm/min was used to 75% of estimated UCS and then control switched to a more sensitive circumferential deformation control with a rate of 0.0125mm/min. The loading rate control is described further in Section 5.2.1. The BTS specimens had a diameter of 76 mm and a consistent thickness to diameter ratio (t/D) of 0.5.

The water content of UCS and BTS specimens was altered using seven methods:

- Immersion saturation for 1 week, 1 month, and 3 months

- Vacuum saturation for 1 week
- Room Relative Humidity (RRH)
- Oven drying for 1 week and 1 month

These saturation methods used a Synthetic Pore Water (SPW) made in accordance to the in situ SPW composition reported for the Cobourg Formation at the Bruce DGR nuclear site by Intera (2010). RRH specimens were stored within the preparation laboratory and were exposed to the environmental conditions present there. Immersion samples were submerged in SPW for periods of one week, one month, and three months. Vacuum saturation involved placing the sample, on its side, in a vacuum chamber while slowly filling the containment vessel until submersion was achieved. Once submerged the sample was held under vacuum for one week. Oven-dried specimens were stored in a forced air oven at 50°C for the duration of one week and one month. Water content measurement for all samples was initiated immediately after testing.

The UCS and Brazilian specimens used to examine the effect of saturation have been listed below in Table 1 and Table 2. The UCS specimen ID nomenclature is such that the first letter and number correspond the block the sample was drilled from, the second number corresponds to the drill hole number in that block, and the third number represents the top (1) or bottom (2) of the core if it broke during coring. The BTS specimen ID nomenclature is such that the first letter and number correspond the block the sample was drilled from, the second number corresponds to the drill hole number in that block, Top corresponds to a specimen sawed from the top of the drill core, Bot corresponds to a specimen sawed from the bottom of the drill core, and the third number corresponds to the first (1), second (2), or third (3) specimen prepared from that same location. The larger the third number, the lower the location of the BTS specimen in the original core (i.e. 1 would be the highest, and 3 the lowest of a set).

Table 1: List of UCS specimens used to examine the effect of saturation

Specimen ID	Saturation State
A2-1-1-U A2-7-1-U A2-12-2-U	Pressure Saturated 1 Week
A2-2-1-U A2-8-1-U A2-13-1-U	Submersion Saturated 1 Week
A2-3-1-U A2-9-1-U A2-14-1-U	Submersion Saturated 1 Month
A2-4-1-U A2-10-1-U A2-14-2-U	Submersion Saturated 3 Months
A2-5-1-U A2-11-1-U A2-15-1-U	Oven-dried 2 Weeks
A2-6-1-U A2-12-1-U A2-15-2-U	Oven-dried 1 Month

Table 2: List of BTS specimens used to examine the effect of saturation

Core ID	Brazilian ID	Saturation State
A2-1-1	A2-1-Top	Pressure Saturated 1 Week
	A2-1-Bot-1	
A2-7-1	A2-7-Top	
	A2-7-Bot	
A2-4-1	A2-4-Top-3	
A2-2-1	A2-2-Top	
	A2-2-Bot	
A2-8-1	A2-8-Top-1	
	A2-8-Bot-1	
A2-13-1	A2-13-Top	
A2-3-1	A2-3-Top	Submersion Saturated 1 Month
	A2-3-Bot	
A2-9-1	A2-9-Top	
	A2-9-Bot	
A2-10-1	A2-10-Top-2	
A2-4-1	A2-4-Top-1	
	A2-4-Top-2	
A2-10-1	A2-10-Top-1	
	A2-10-Bot-1	
	A2-10-Bot-2	
A2-5-1	A2-5-Top	Oven-dried 2 Weeks
	A2-5-Bot	
A2-11-1	A2-11-Top-1	
	A2-11-Bot-2	
	A2-11-Top-2	
A2-6-1	A2-6-Top	
	A2-6-Bot	
A2-8-1	A2-8-Top-2	
	A2-8-Bot-2	
A2-1-1	A2-1-Bot-2	

The influence of specimen scale was investigated by testing 12 UCS and 17 BTS specimens with four different diameters. The diameter of the specimens varied between 50 mm, 76 mm, 101 mm, and 127 mm. The L/D remained at 2.5 for all UCS specimens, and all BTS specimens had a t/D of 0.5. The UCS and Brazilian specimens used to examine the effect of scale have been listed below in Table 3 and 4

Table 3: List of UCS specimens used to examine the effect of scale

Specimen ID	Specimen Diameter
C1-6-1-U C1-8-1-U C1-13-1-U	50 mm
C1-4-1-U C1-9-1-U C1-12-1-U	76 mm
B1-1-1-U B2-1-1-U B2-2-1-U	101 mm
C1-1-1-U C1-5-1-U2 C1-10-1-U	126 mm

Table 4: List of BTS specimens used to examine the effect of scale

Core ID	Brazilian ID	Specimen Diameter
C1-6-1	C1-6-1	50 mm
	C1-6-2	
C1-8-1	C1-8-1	
	C1-8-2	
C1-13-1	C1-13-1	
C1-4-1	C1-4-Bot-1	
	C1-4-Bot-2	
C1-2-1	C1-2-Top	
C1-12-1	C1-12-Top	
	C1-12-Bot	
B1-1-1	B1-1-Top-1	101 mm
B2-1-1	B2-1-Top-1	
	B2-1-Top-2	
B2-2-1	B2-2-Top-1	
C1-1	C1-1	126 mm
C1-5	C1-5	
C1-10	C1-10	

The influence of loading rate was examined using 24 UCS specimens loaded to failure within different time periods. The UCS specimens had a diameter of 76 mm and a consistent L/D of 2.5. In addition to the 20 minute time to failure suite, specimens were loaded to failure in four target time periods:

- 2 minutes
- 6 minutes
- 60 minutes
- 600 minutes

In addition, half of the specimens were submerged in the SPW for a period of one month prior to testing. This was done to further investigate the influence of saturation and examine its time dependent relationship to the geomechanical properties of Cobourg limestone. The UCS specimens tested under varying loading rates (times to failure) have been listed below in Table 5. The 20 minute RRH and 1 month saturated samples in the previous suite of testing are also included in this comparison. The corresponding deformation rates for control are discussed in Section 5.2.1.

Table 5: List of UCS specimens used to examine the effect of loading rate

Specimen ID	Loading Rate	Saturation State
A1-7-1-U C2-4-2-U A1-11-1-U	Specimens are failed in 2 min	Room RH
A1-3-1-U2 C2-2-1-U A1-5-1-U	Specimens are failed in 6 min	
A1-8-1-U C2-8-1-U A1-12-1-U	Specimens are failed in 60 min	
A1-4-1-U C2-3-1-U A1-9-1-U	Specimens are failed in 600 min	
A1-7-2-U C2-15-1-U A1-16-1-U	Specimens are failed in 2 min	
A1-3-2-U C2-11-1-U C2-12-2-U	Specimens are failed in 6 min	1 Month Submersion Saturated
A1-8-2-U C2-16-1-U C2-4-1-U	Specimens are failed in 60 min	
A1-4-2-U C2-14-1-U A1-15-1-U	Specimens are failed in 600 min	

Failure of the specimens was controlled using axial and circumferential strain based on continuous readout from the equipped extensometers. The axial and circumferential strain rates were adjusted such that the specimen would reach peak strength at the targeted time period.

4. SPECIMEN PREPARATION

The previously listed Uniaxial Compressive Strength (UCS) and Brazilian Tensile Strength (BTS) specimens have been prepared for testing using ASTM standards (references), and will be referenced where applicable. The ISRM Suggested Methods or major scientific publications are used when ASTM standards are not available or sufficient in addressing the employed procedure within the testing framework.

4.1 Sample Collection

Large blocks of Cobourg limestone were obtained by McGill University from Saint Mary's Quarry located in Bowmanville, Ontario. The quarry uses the in situ Cobourg for aggregates and cement manufacturing, meaning there are no constraints on the quality of retrieved samples. Blocks of Cobourg are excavated by blasting, likely subjected to blast. The blocks selected for this study were taken from the upper part of Bench 2 where the blast holes were stemmed (no explosives) to minimize the damage sustained during blasting. During retrieval of the blocks the quarry excavation level was approximately 70 m below ground level (Figure 1). Two blocks of rock were chosen based on size and weight restrictions related to transportation from the quarry to Montreal. The rocks were selected based on the absence of visible fractures, visibility of stratification, the presence of squared rock faces, and weight.



Figure 1: Saint Mary's Quarry. Sample location shown by black arrow

The largest block selected was approximately 0.8 m wide and 3.18 m long, while the smaller block is approximately 0.9 m wide and 2.4 m long. The blocks were measured in order to identify the most suitable cutting pattern to create more manageable pieces. The cutting was conducted by Pierrexpert, Montreal due to their ability to handle and cut both the larger and smaller blocks. The cutting was done using a water-cooled flexible chain saw, as shown in Figure 2. The preparation of smaller blocks was carried out under continuous supervision and low cutting speeds were maintained in order to minimize sample disturbance. Six cubes were cut with side lengths of 400 mm and were made available by McGill University. The blocks were then transported to the Queen's Geomechanics Group Testing facility in Kingston, Ontario for core drilling.



Figure 2: Water-cooled cutting of Cobourg blocks using a flexible chain saw at Pierrexpert, Montreal

4.2 Drilling, Cutting, Grinding

The UCS samples are prepared in accordance with the ISRM suggested methods for Unconfined Compressive Strength Testing (Fairhurst and Hudson, 1999) and the ASTM D4543 standard (ASTM 2008a), where applicable. The BTS specimens are prepared in accordance with ASTM D3967 (2008b).

The Cobourg limestone blocks are drilled with a Kitchen-Walker 4' radial drill using diamond core bits. The top surface of the blocks is marked for drilling location and core bit size to be used (Figure 3a). The blocks are then secured in place (Figure 3b) to minimize disturbance during drilling for maximum quality of the cores. The rotation and spindle speed of the drill is adjusted according to the rock and core bit to maximize the quality and smoothness of the circumferential surface of the cores. An example for drilling a 400 mm cube of the Cobourg limestone is shown in Figure 3c.

The cores are cut into UCS and BTS test specimens with a diamond saw (Figure 4a). The UCS specimens are cut to the final length of the specimen with an additional length of 2 to 3 mm for grinding. If the length of the cores permits, BTS specimens are also cut from the top and bottom of the UCS specimens. When cutting BTS specimens, special care is taken to ensure that the ends remain parallel to one another and meet the ASTM D3967 (2008b) standard, as listed in Section 4.3.2. The UCS specimens, after cutting, are ground down to the proper size with a GCTS RSG-200 specimen grinder (Figure 4b). The specimens are ground with a diamond grinding cup-wheel in order to meet the required flatness of the two ends as well as the perpendicularity of the two ends with respect to specimen axis, as listed in Section 4.3.1.

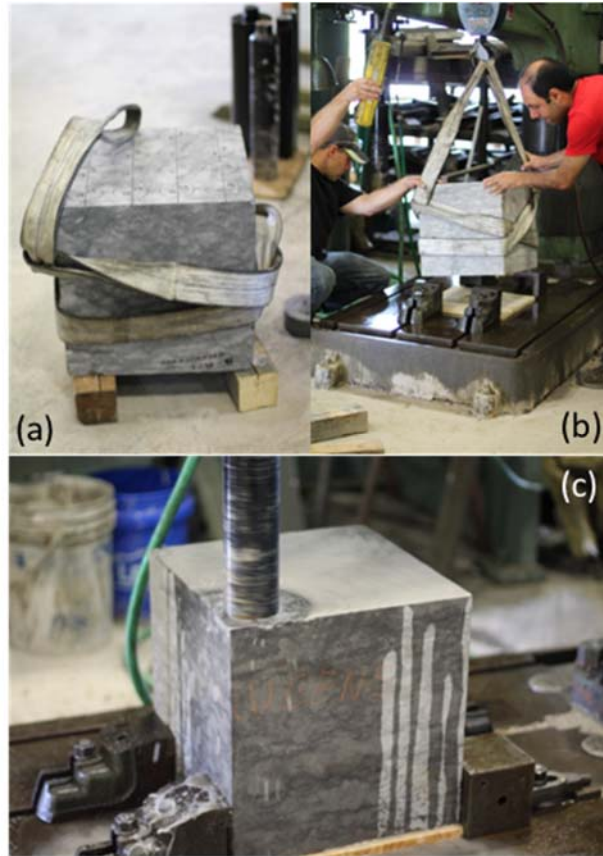


Figure 3: (a) Marking the drilling location and size on top of the Cobourg limestone blocks, (b) securing the block at the base of the drilling machine, (c) drilling a Cobourg limestone block

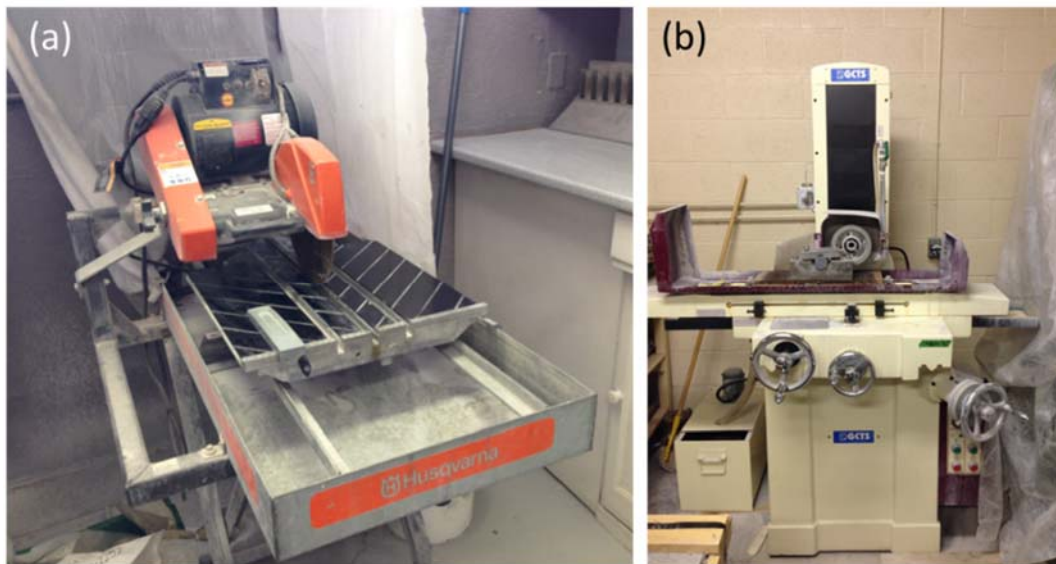


Figure 4: (a) Diamond saw for cutting cores, (b) Specimen grinder with diamond grinding cup-wheel

4.3 Verification of Dimensions

4.3.1 UCS Specimens

The UCS specimens are drilled, cut and grinded flat to meet the tolerances as specified by ASTM D4543 (2008a). The dimension tolerances include:

- Smoothness of the cylindrical surface of the specimen shall be within 0.50 mm over the full length of the specimen
- Smoothness of the end surfaces shall not exceed 25 μm
- The perpendicularity of the specimen ends to the axis of the specimen shall not depart from a right angle by more than 0.25°
- The angular difference for parallelism of the opposing specimen ends of a specimen shall not be more than 0.25° for spherically seated test machines and 0.13° for fixed end test machines

The UCS specimens are prepared with the length to diameter (L/D) ratio of 2.5 to meet the requirements of both ASTM D4543 (2008a) as well as the ISRM suggested methods (Fairhurst and Hudson, 1999) which recommend a L/D ratio of 2-2.5 and 2-3, respectively. An Inspection Grade (Grade A) granite support surface, a digital indicator with 0.001 mm resolution, a V-block, a feeler gage set, and an electronic caliper are used for the verification of tolerances and dimensions of the specimens (Figure 5).



Figure 5: Granite support surface, digital indicator, V-block, feeler gage, and the electronic caliper used for verification of the specimen dimensions

The length and diameter of the specimens are determined in accordance with ASTM D4543 (2008a) and ISRM suggested methods (Fairhurst and Hudson, 1999) using an electronic caliper. The length is determined to the nearest 0.01 mm by taking an average of two lengths measured perpendicular to each other from the center of the end faces. The diameter is determined to the nearest 0.01 mm by taking the average of two diameters measured perpendicular to one another close to the top, middle, and bottom of the

specimen. The accuracy of the length and diameter measurements meets and exceeds the requirements of ASMT D4543 (2008a) and ISRM suggested methods (Fairhurst and Hudson, 1999).

The smoothness of the cylindrical surface of the specimens are verified by sliding the specimens along their axial axis on a V-block and measuring the maximum deviation. The perpendicularity of the specimen ends to the axis of the specimen is verified by means of a feeler gage set and measuring the maximum distance of one end of the specimen from a flat vertical block when the other end is pushed tight against the same block. The flatness of the specimen ends and their parallelism is verified by doing measurements along two perpendicular diameters at the two ends of the specimen at 10 mm intervals (higher resolution measurements, 5 mm intervals, are also performed for randomly selected specimens). An example is shown in Figure 6.

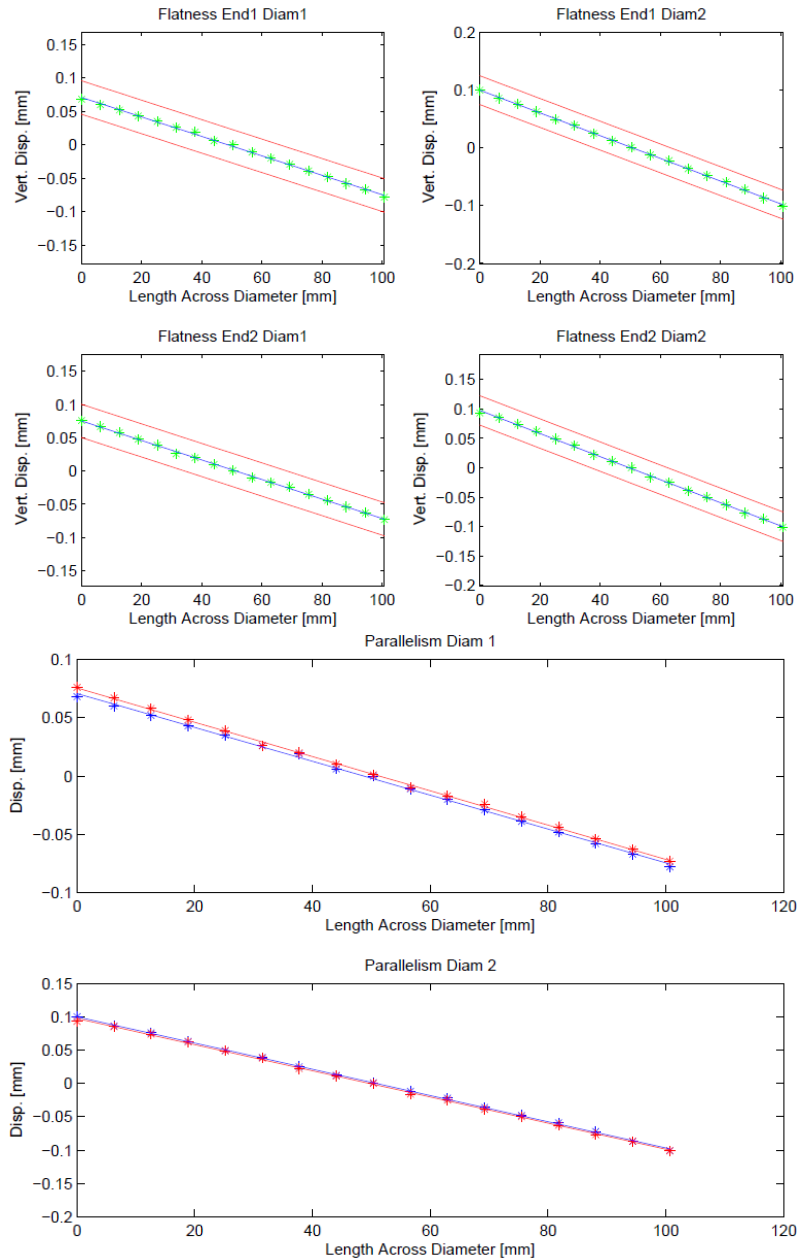


Figure 6: Verification of the flatness and parallelism of the specimen ends.

4.3.2 BTS Specimens

The BTS specimens are drilled, cut, and then inspected to meet the tolerances specified by ASTM D3967 (2008b). The dimension tolerances include:

- Smoothness of the cylindrical surface of the specimen shall be within 0.50 mm over the full length of the specimen
- The perpendicularity of the specimen ends to the axis of the specimen shall not depart from a right angle by more than 0.5°

The BTS specimens are prepared with the thickness to diameter (t/D) ratio of 0.5 to meet the requirements of ASTM D3967 (2008b), which specifies a ratio of 0.2-0.75. An Inspection Grade (Grade A) granite support surface, a digital indicator with 0.001 mm resolution, a V-block, a feeler gage set, and an electronic caliper are used for the verification of tolerances and dimensions of the specimens (Figure 5).

The diameter and thickness of the specimens is determined to the specifications of ASTM D3967 (2008b) using the electronic caliper. The diameter is determined to the nearest 0.01 mm using an average of three measurements, one of which is along the loading diameter. The thickness is determined to the nearest 0.01 mm using an average of three measurements, one of which is at the center of the disk. The accuracy of the length and diameter measurements meets and exceeds the requirements of ASMT D3967 (2008b). The smoothness of the cylindrical surface of the specimens is verified by sliding the specimens along their axial axis on a V-block and measuring the maximum deviation. The perpendicularity of the specimen ends to the axis of the specimen is verified by means of a feeler gage set and measuring the maximum distance of one end of the specimen from a flat vertical block when the other end is pushed tight against the same block.

4.4 Photography and Scanning

4.4.1 Blocks

The limestone blocks are photographed before drilling in different orientations for generation of the 3-Dimensional photogrammetric model of the blocks. Similar procedure is repeated for each block while the surface of the block is moistened for better appearance of the geologic features.

4.4.2 Cores

Drilled cores are photographed in dry and wet (surface) conditions at 45° radial increments (8 photos per core for each of the wet and dry conditions). Examples are shown in Figure 7.



Figure 7: Drilled cores are photographed in dry and wet (surface) conditions

4.4.3 Specimens

The prepared BTS and UCS specimens are photographed in dry condition at 90° radial increments (four photos per specimen, Figure 8a). The top and bottom of BTS specimens is also photographed to record and identify any potential features that could influence results (Figure 9). Each UCS specimen is scanned with a cylinder scanner (Figure 10) that was designed and built at the Queen's Geomechanics Group. The scanner provides an unrolled view of the specimen without any optical distortion for image analysis of the clay content of the specimens (Figure 8b).

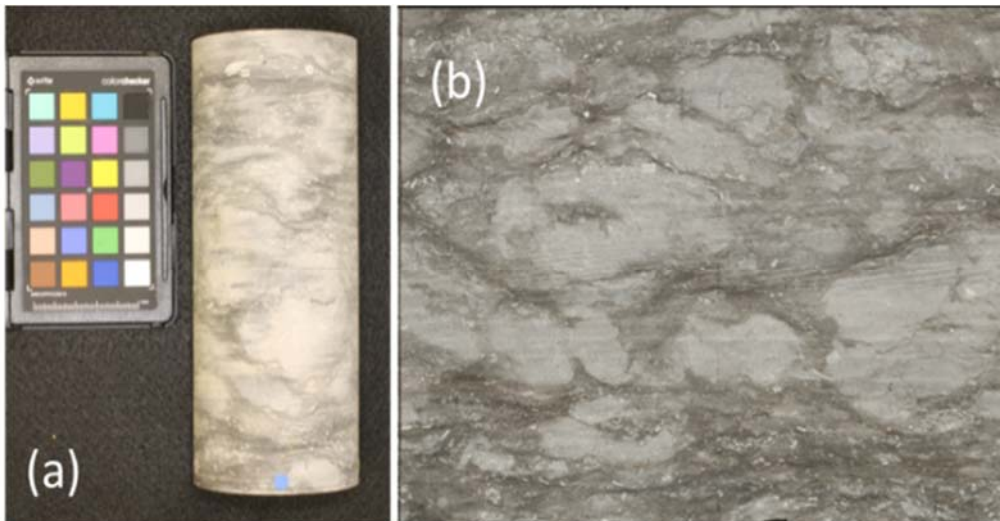


Figure 8: (a) One of the four sides of prepared specimens are photographed at 90° radial increments before testing, (b) an example for an unrolled image of a Cobourg limestone circumferential surface produced by the cylinder scanner.



Figure 9: Photograph of the bottom of two prepared BTS specimens

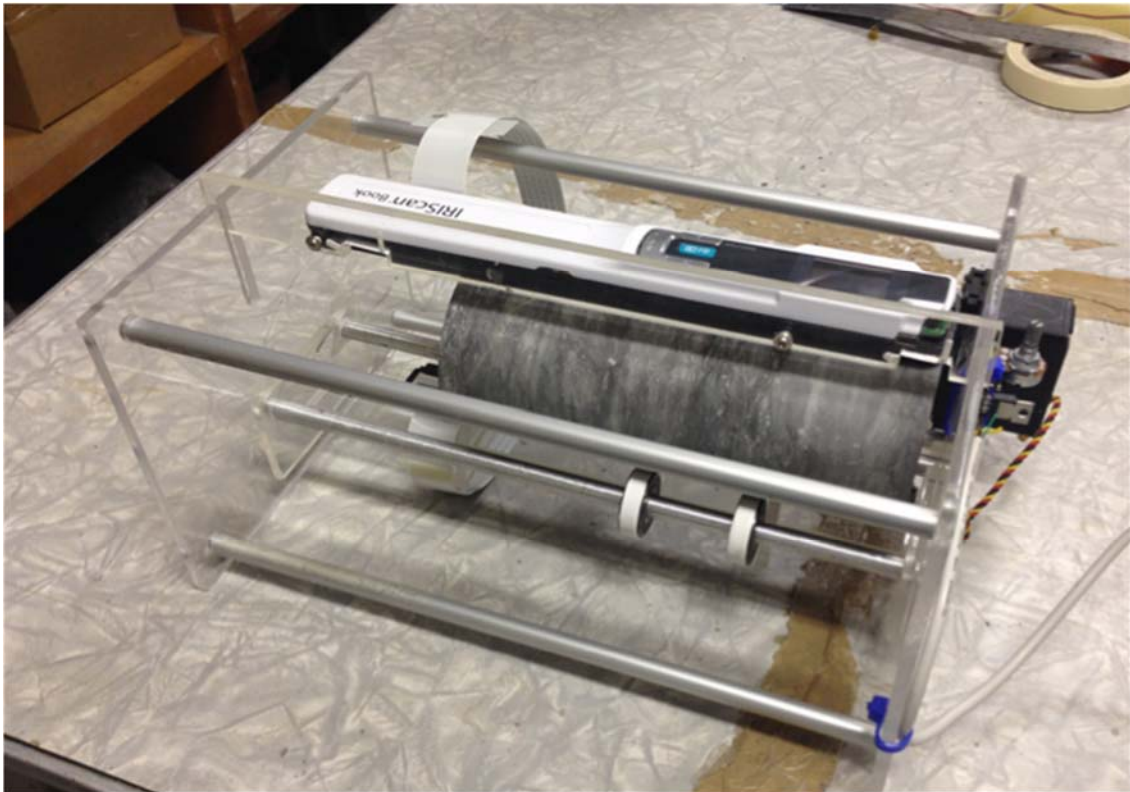


Figure 10: Cylinder scanner used for capturing the unrolled circumferential surface of the specimens

4.4.4 Test Setup

The testing set-up for each specimen is photographed before testing. For specimens with visible fractures, the image of their post-test state is also captured.

4.5 Saturation and Drying Methods

Synthetic Pore Water (SPW) is used for saturation of the specimens. The SPW solution is made in the laboratory according to the SPW composition reported for limestone by Al et al. (2010). Two types of saturation techniques are employed: submerging and vacuum saturation. In the submerging saturation technique, the specimens are submerged in the SPW fluid within a container with tight lid to avoid evaporation and consequently changes in the SPW composition. The submersion duration for the specimens vary depending on the testing protocol. The vacuum saturation of the specimens is performed by using a set of stainless steel trays, a vacuum chamber, and vacuum pump as shown in Figure 11.



Figure 11: Apparatus used for vacuum saturation of the specimens

There is no standard method available for vacuum saturation of low porosity rocks, therefore a procedure has been adapted based on Dunning & Yeskis (2007) and ISRM (1979). In the developed approach, Stainless steel trays were stacked and a half millimetre diameter hole was drilled into the top tray to allow the SPW fluid to drip into the bottom tray (Figure 12).



Figure 12: Stainless steel trays used during vacuum saturation

The amount of fluid that is needed to fill the bottom tray while containing the specimen(s), ensuring they become fully submerged is calculated. The specified amount of SPW fluid is then transferred to the top tray while the hole is plugged. The top tray is then placed into the angle brackets of the bottom tray which already contains the specimen(s). Both trays are then placed into the vacuum chamber and the hole in the middle of the top tray is unplugged allowing for the SPW fluid to drip into the bottom tray slowly. Then the vacuum chamber exhaust valve is sealed and the vacuum pump is turned on, bringing the suction in the vacuum chamber to 700 mmHG below atmospheric pressure. The suction pressure is maintained in the chamber during saturation time (one week).

Drying of specimens is performed in a VWR forced air oven (Figure 13) at 50°C to avoid inducing heating-related fractures in the specimens or cooking the clay in the Cobourg limestone. During drying specimens are placed directly on the stainless steel racks in the oven and held there until the designated time period has been reached. The specimens are removed just before testing, to maintain the established water content.



Figure 13: VWR oven used to dry UCS and BTS specimens

4.6 Water Content and Bulk Density Measurements

The density of the specimens is calculated after preparation but before testing with the moisture content corresponding to the relative humidity of the room, according to the equations in ISRM (1979). Water content of the specimens is measured after testing according to ASTM D2216 (2010). Specimens are dried in a VWR forced air oven at 50°C for a minimum duration of a month. Their mass is measured regularly and specimens are removed from the oven when the change in their mass is less than 0.5 g within a week. A VWR scale with a capacity of 6000 g and readability and repeatability (Std. Dev.) of 0.01 g is used for density and water content related mass measurement of the specimens.

5. TESTING CONFIGURATION AND PROCEDURES

The Uniaxial Compressive Strength (UCS) and Brazilian Tensile Strength (BTS) specimens utilize much of the same testing system, however, there are some differences in their equipment, configuration, and testing procedure. The following sections of this report will provide details regarding the MTS 815 Testing system used to perform UCS and BTS tests, as well as additional equipment, testing configurations, and testing procedures for both test types.

5.1 Equipment

5.1.1 MTS 815 Rock Mechanics Testing System

The UCS and BTS tests are performed with a MTS 815 Rock Mechanics Testing System that is a closed-loop, computer-controlled, servo-controlled hydraulic compression machine (Figure 14).



Figure 14: MTS rock mechanics testing system at the Queen's Geomechanics testing laboratory

The system consists of:

- MTS 315.02 load frame with 2700 kN compression rating, including a differential pressure (ΔP) transducer (which monitors the difference in pressure on each side of the actuator piston and is calibrated to represent the force output of the actuator) - Certificate of Calibration in Appendix 1
- MTS Model 505.07 Silent Flo Hydraulic Power Supply
- MTS FlexTest 60 controller
- MTS triple averaging axial extensometer with overall axial travel distance of ± 4.0 mm and gauge length of 50.0 mm (Certificate of Calibration in Appendix 2)
- Circumferential extensometer with ± 4.0 mm travel connected to a roller chain (Certificate of Calibration in Appendix 3)
- Computer with the MTS controlling software

5.1.2 Acoustic Emission (AE) Monitoring System

The AE activity of all UCS specimens during testing are monitored for further micro-cracking information. A Physical Acoustics Corporation (PAC) Pocket AE system connected to two PAC R15 sensors with an operating frequency [resonant frequency] of 50-400 [75] kHz is used (Figure 15). The parametric input to the Pocket AE allows for recording of the axial force from the MTS test system as an external channel to synchronize the AE data with the axial stress applied to the specimens.

In all tests on the Cobourg limestone the channel sensitivity threshold is set to 30 dB and the Pocket AE's built in pre-amplifier is enabled. The waveforms are sampled at a rate of 10 MSPS (Mega Samples per Second). The High pass and the Low Pass analog filters are set to 20 kHz and 1 MHz, respectively.

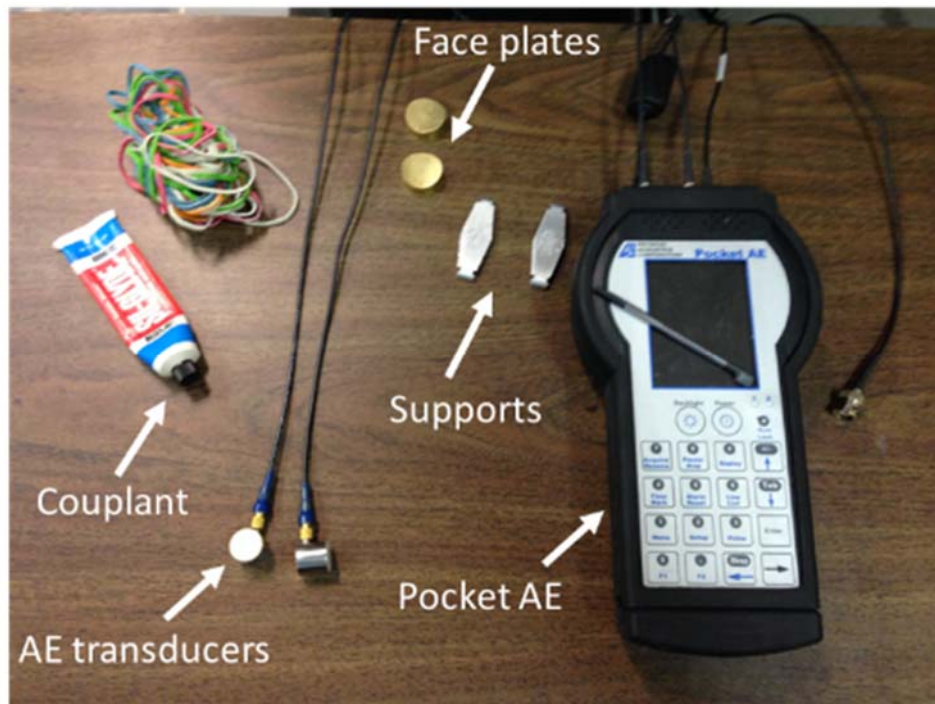


Figure 15: PAC Pocket AE monitoring system, PAC R15 sensors, and accessories

5.1.3 Strain Gauges

Strain gauges were utilized on a number of BTS tests in order to investigate the use of strain gauges as an alternative to extensometers, and assess the best technique for future testing. The strain gauges used are 120 Ohm HBM strain gauges with a gauge length of 10 mm. The gauges connect to a four channel amplifier which directly connects to the input channels of the MTS FlexTest 60 controller. This is done so that the collected strain data can be synced with the applied load data. The sampling rate for Brazilian tests is set 10 Hz, providing continuous strain readout during testing. Additional specifications of the HBM strain gauges have been included in Appendix 4.

5.2 UCS Testing Procedure

In all UCS tests on the Cobourg limestone, axial deformation is measured with the three averaging direct contact extensometers (50.0 mm gauge length). The extensometers are held in place by the contact force provided from six mounting springs, with elastic bands replacing the springs for tests with fast loading rates. Circumferential deformation is measured by means of an extensometer connected to a roller chain wrapped around the circumference of the specimen at its mid-height. The applied force to the specimen is measured with the (ΔP) transducer. The applied force and the deformation data from the sensors are recorded with the frequency of 4 Hz during the tests. Non-lubricated steel platens, fixed at the bottom and with spherical seat on top, are used for the UCS tests. Larger platens made of hardened steel are placed over the pre-existing platens for the largest diameter (126 mm) tests. Figure 16 shows the setup of a UCS test.

Acoustic emissions are monitored in all UCS tests on the Cobourg limestone. The two AE transducers are secured on the circumference of the specimens, between the extensometers and outside the mounting spring (used for extensometers) by means of aluminium supports and elastic bands. Brass face plates are used to fit the curved circumferential surface of the specimens to flat surface of the AE transducers. Sil-Glyde lubricating compound is used as the couplant for a better wave transfer between the surface of the specimens to transducers.

The UCS tests are started under the axial deformation control and then switched to the circumferential deformation control at 75 MPa to ensure a controlled test in the post-peak region. A detailed testing routine that conforms with ASTM D7012 (2014) and ISRM suggested methods (Fairhurst and Hudson, 1999) is used and is listed below:

1. Raise the specimen manually to near contact with the top platen
2. Zero the readings of axial force as well as axial and circumferential extensometers
3. Start the programmed test control routine
4. Raise the specimen to contact with the top platen, then:
 - Move the actuator up with the rate of 0.1 mm/min
 - Stop when the applied force reaches 5.0 kN
 - Reduce the applied force 1.0 kN with the unloading rate of 10 kN/min
5. Start recording the applied force, axial and lateral deformations, and AE activity
6. Start the test in axial deformation (axial extensometer) control mode with the rate ranging between 0.1 to 0.0003 mm/min depending on the testing protocol
7. When the applied stress reaches 75.0 MPa switch the test control mode to circumferential strain control
8. Continue loading the specimen corresponding to the circumferential deformation ranging between 0.125 to 0.000375 mm/min depending on the testing protocol
9. Stop the test when the applied force to the specimen in the unloading region reaches 60% of the maximum applied force to the specimen during the test

The relative humidity of the room as well as the temperature is recorded at the beginning of each test. The specimens are visually inspected at the beginning of the test and any type of structural weakness (e.g. healed fractures) are recorded for the specimen. The mode of failure for each test is recorded as well.

5.2.1 Axial and Circumferential Deformation Rates

The ASTM standard recommends a failure time of up to 15 minutes for standard geotechnical samples (50-54mm diameter). The standards refer to time-to-failure rather than a mandated strain or displacement rate. A baseline testing time-to-failure of 20 minutes was selected for the 76mm samples in this investigation.

The axial displacement control (0.01mm/min for a 76mm diameter sample or a 5.3E-5/min strain rate) was switched to circumferential control at 75MPa (75% of minimum UCS anticipated) to allow more precise control of the near yield and post yield behaviour. It has been found that the lateral (circumferential) strain rate just prior to failure (between CD and peak UCS) can be over 4 times the elastic rate due to crack formation and dilation. In order to provide a lateral deformation control value that, at the point of failure would be equivalent to maintaining the initial axial strain rate a circumferential displacement rate of 0.0125mm/min was selected. For other sample sizes, the axial loading rate was kept constant through the elastic range for simplicity but the lateral displacement rate was adjusted for the sample diameter.

All 76mm saturation trial specimens have been tested at the standard axial and circumferential deformation rates, 0.01 and 0.0125 mm/min, respectively. The deformation rates for the loading rate trial specimens have been adjusted to ensure that the specimen will fail in the targeted time period. The scale effect tests have the same axial deformation rate (0.01 mm/min) but different circumferential deformation rates. This is done to account for the difference in the size of the specimen and maintain a constant axial strain rate. The deformation rate used in each test has been summarized in Table 6.

Table 6: Axial and circumferential deformation rates used for each test type

Test Type	Axial Deformation Rate (mm/min)	Circumferential Deformation Rate (mm/min)
Saturation	0.0100 (76mm, 20 mins)	0.0125
50 mm Diameter	0.0100	0.00825
76 mm Diameter	0.0100	0.0125
101 mm Diameter	0.0100	0.0165
126 mm Diameter	0.0100	0.021
2 min Failure Target	0.1000 (76mm)	0.125
6 min Failure Target	0.0300 (76mm)	0.0375
60 min Failure Target	0.0030 (76 mm)	0.00375
600 min Failure Target	0.0003 (76mm)	0.000375

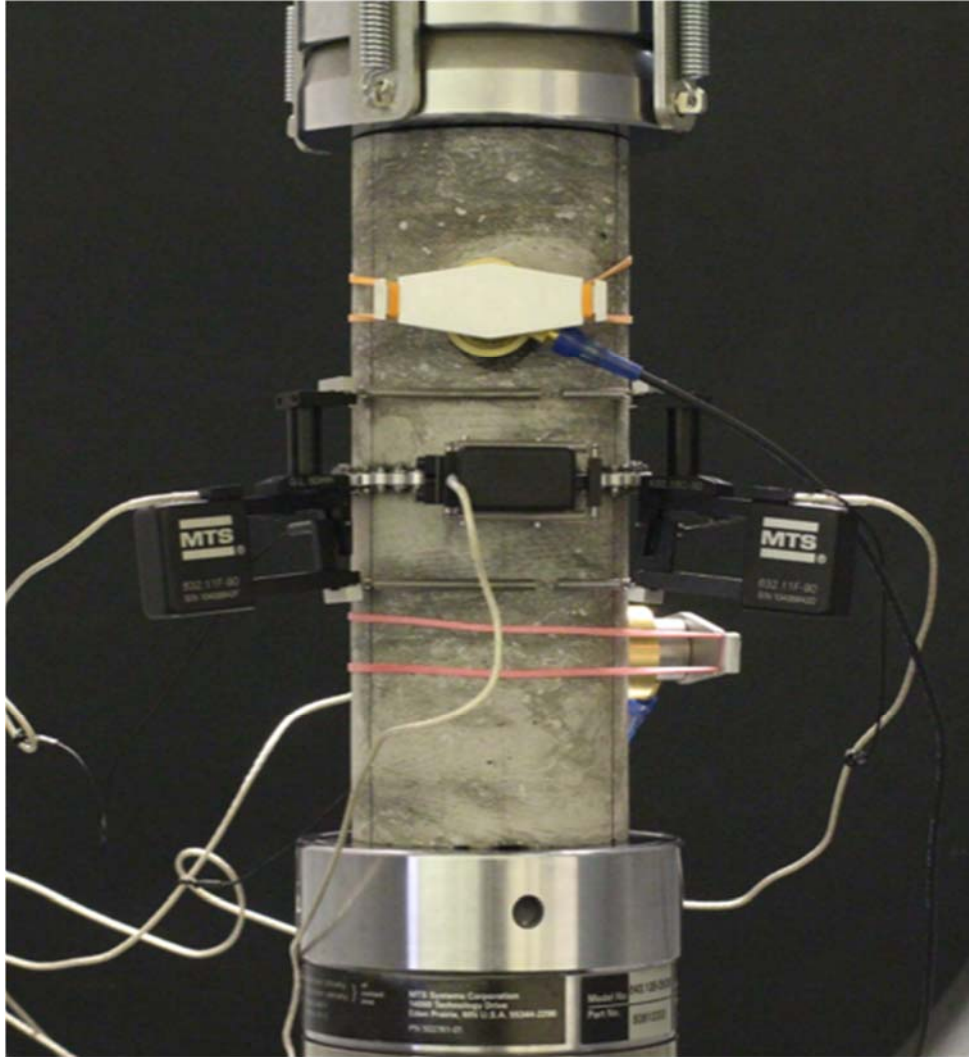


Figure 16: UCS test set-up for Cobourg limestone specimens

5.3 BTS Testing Procedure

In 35 of the BTS tests lateral deformation is measured with two of the averaging direct contact extensometers (20.0 mm gauge length). The third extensometer is connected to the system, however, with the zero-displacement pin remaining in to provide no influence on readings. This is required as the MTS system requires feedback from all three extensometers to operate. The extensometers are held in place by the contact force provided by elastic two elastic bands wrapped around each specimen (Figure 17a). The extensometers are positioned at the centre of the specimen's face, aligned perpendicular to the loading direction. Strain gauges were used to record lateral deformation measurements of the 12 other BTS tests. A strain gauge with foil length of 10 mm was placed at the center of each specimen face, for a total of two gauges per specimen. The gauges were aligned perpendicular to loading direction and are held in place using a cyanoacrylate adhesive (Figure 17b).

The applied force to the specimen is measured with the (ΔP) transducer. The applied force and the deformation data from the sensors are recorded with 10 Hz frequency during the tests. Curved bearing blocks made of hardened steel are used for the 50 and 76 mm BTS

tests to reduce the contact stresses (Figure 17). The upper bearing block has a spherical seat formed by a half ball bearing. The larger BTS tests (101 and 126 mm) use non-lubricated steel platens, fixed at the bottom and with a spherical seat on top. Wooden senior tongue depressors are cut to size and used as cushions between the platens and the specimen to reduce the contact stress (Figure 18).

The BTS tests are conducted under monotonically increasing load until the specimen has failed. A testing routine that conforms with ASTM D3967 (2008b) is used and is detailed below:

1. Place the specimen in the center of the curved bearing blocks or platens
2. Raise the specimen manually to near contact with the top platen
3. Zero the readings of axial force and extensometers or strain gauges
4. Start programmed test control routine
5. Raise the specimen to contact with the top platen, then:
 - Move the actuator up with the rate of 0.1 mm/min
 - Stop when the applied force reaches 5.0 kN
 - Reduce the applied force to the specimen to 1.0 kN with the unloading rate of 10 kN/min
6. Start recording the applied force and lateral deformations
7. Start the test in load control mode with the rate ranging between 0.1 to 0.25 kN/s depending on the diameter of the specimen
8. Stop the test when the applied force to the specimen in the unloading region reaches 60% of the maximum applied force to the specimen during the test

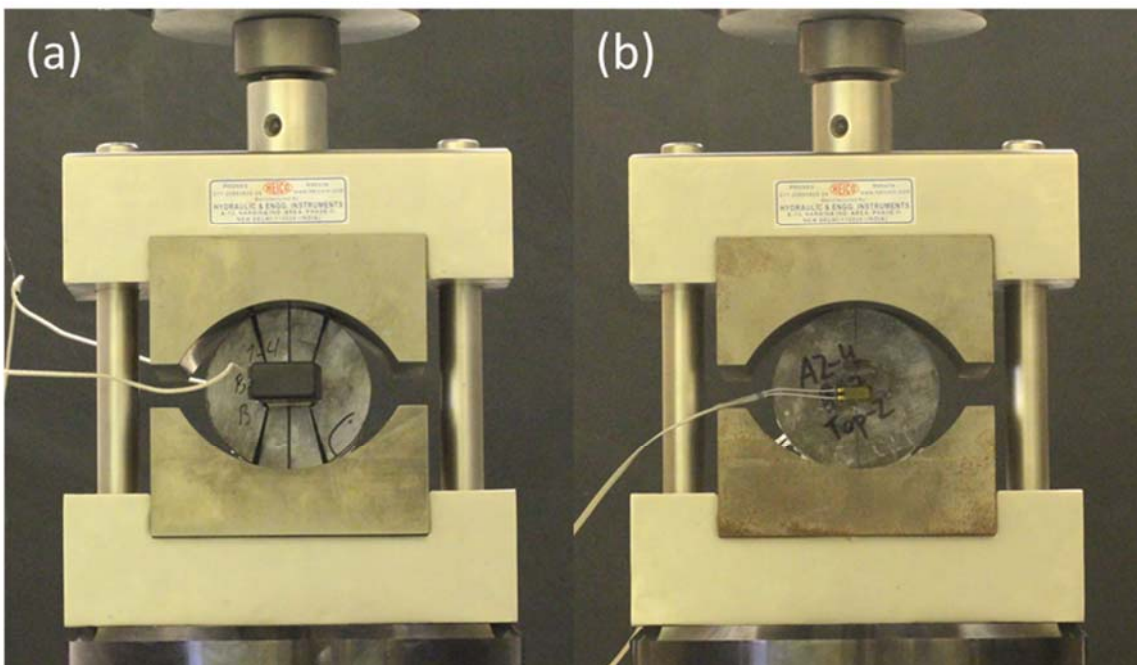


Figure 17: BTS test set-up for 50 and 76 mm Cobourg limestone specimens

The relative humidity of the room as well as the temperature is recorded at the beginning of each test. The specimens are visually inspected at the beginning of the test and any type of structural weakness (e.g. healed fractures) are recorded for the specimen. The mode of failure for each test is recorded as well.

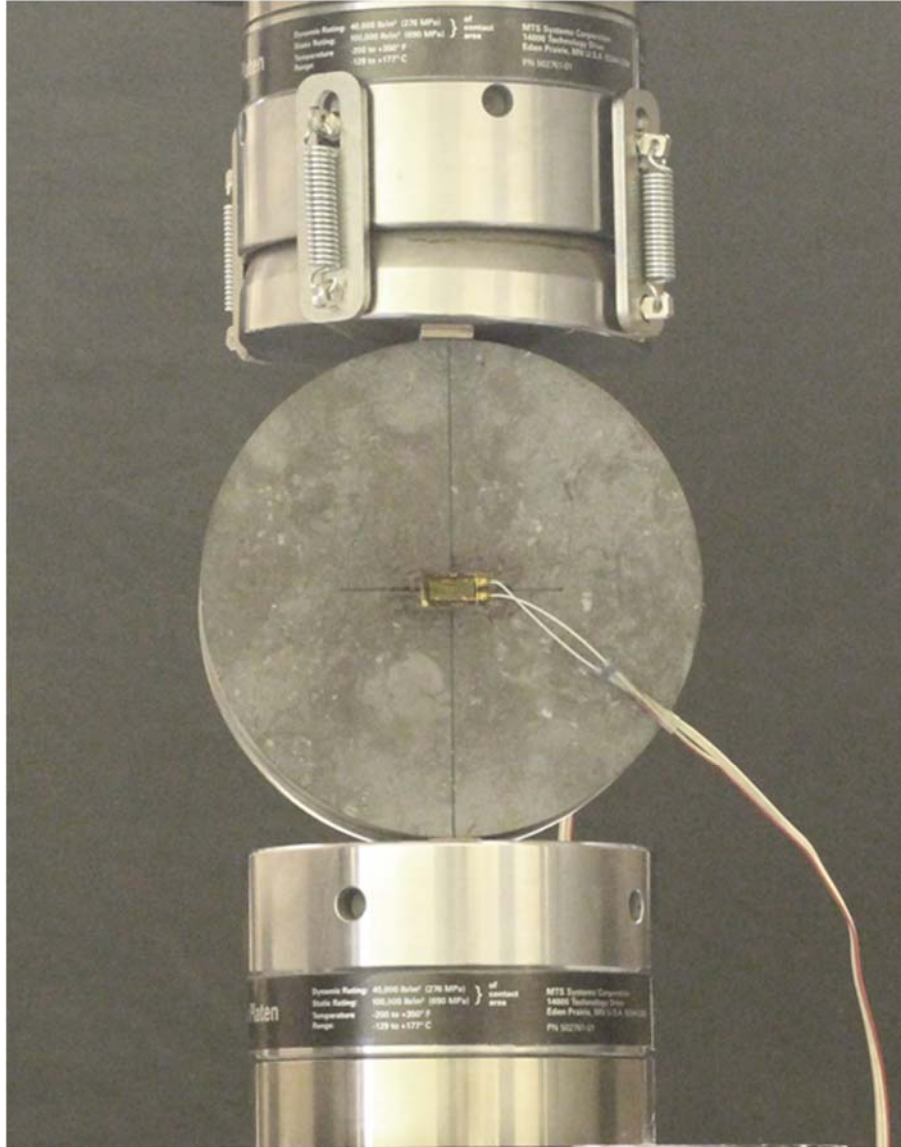


Figure 18: BTS test set-up for 101 and 126 mm Cobourg limestone specimens

6. DATA PROCESSING METHODOLOGY

The data collected during testing is used to calculate various geomechanical properties using standardized ASTM methods. The ISRM Suggested Methods or major scientific publications are used when ASTM standards are not available or sufficient in addressing the employed procedure within the testing framework. In addition, Crack Initiation (CI) and Critical Damage (CD) thresholds have also been estimated using six different methods. The methods used to calculate these properties have been described in the following subsections.

6.1 Water Content

The water content by mass of each specimens is calculated once the final dried mass has been measured and according to ASTM D2216 (2010). The water content is recorded to the nearest 1% and is calculated using Equation 1:

$$w = \left(\frac{M_{cms} - M_{cds}}{M_{cds} - M_c} \right) \times 100 \quad [1]$$

where w is water content (%), M_{cms} is the mass of the container and moist specimen (g), M_{cds} is the mass of the container and oven-dried specimen (g), and M_c is the mass of the container (g).

6.2 Bulk Density

The bulk density of each specimen is calculated according to ISRM (1979), using Equation 2:

$$\rho = \frac{M}{V} \quad [2]$$

where ρ is the bulk density (kg/m^3), M is the mass of the specimen measured prior to testing (kg), and V is the volume of the specimen calculated from dimensions measured during sample preparation (m^3).

6.3 Elastic Parameters

Young's modulus (E_{50}) and Poisson's ratio (ν_{50}) is calculated for every Uniaxial Compressive Strength (UCS) test using the ASTM D7012 (2014) standard. Young's modulus, E , is defined as the average slope of the straight-line portion of the stress-strain curve, calculated between 40 and 60 percent of the maximum applied load (Equation 3a). The change in stress within this range is divided by the change in strain. Poisson's ratio, ν , is calculated from Equation 3b:

$$E = \frac{\text{Change in axial stress}}{\text{Change in axial strain}} \text{ over interval 30 – 50\% of UCS} \quad [3a]$$

$$\nu = \frac{\text{Change in lateral strain}}{\text{Change in axial strain}} \text{ over interval 30 – 50\% of UCS} \quad [3b]$$

While E_{50} and ν_{50} represent the standard values normally reported, this range of behaviour overlaps with the onset of damage initiation (see Section 6.6) and is therefore subject to inelastic influences.

In this report E35 and ν_{35} are also reported and are the values plotted for the elastic constants (same as in Equations 3 but taken from 25-35% of UCS) in order to obtain a more accurate estimate of true elastic parameters. This care is necessary to ensure accurate calculation of CI. Care is taken to ensure that the 25% lower bound for the measurement range does not include any initial non-linearities due to pre-existing sample damage.

For routine testing in commercial laboratories, it may be prudent to use E40 and ν_{40} as the specified data to be reported for this purpose. While 35% of UCS represents a more accurate sampling point (particularly for Poisson's Ratio) 40% of UCS may be a more robust compromise to ensure that early non-linearity due to seating and damage, that may go undetected, does not influence the results. The values at 50% should be reported to conform to the conventional standards (For this work they are included in the appendix), best practice would dictate either 35% or 40% elastic values be reported as well for use in damage calculations and other applications. Values at 35% are reported in the main body of this report.

6.4 Uniaxial Compressive Strength (UCS)

The UCS of the specimens is calculated according to ASTM D7012 (2014), using the relationship in Equation 4:

$$UCS = \frac{P}{A} \quad [4]$$

where P is the failure load (N), and A is the cross-sectional area (mm²).

6.5 Brazilian Tensile Strength (BTS)

The tensile strength of the Brazilian specimens is calculated according to Equation 5, provided in ASTM D3967 (2008b):

$$\sigma_t = \frac{2P}{\pi LD} \quad [5]$$

where σ_t is the is the BTS (MPa), P is the maximum applied load (N), L is the thickness of the specimen (mm), and D is the diameter of the specimen (mm).

6.6 Crack Initiation (CI) and Crack Damage (CD) Estimation

A variety of methods have been utilized to estimate the crack damage thresholds (CI and CD) based on the stress, strain, and AE data obtained during UCS testing. The strain based methods approximate CI and CD values using axial, circumferential, and volumetric strain data calculated using sample dimensions and displacements measured during testing. The AE methods estimate CI and CD by measuring the rate, amplitude, and duration of AE events during the UCS test. All methods used to analyze the crack damage thresholds of Cobourg limestone in this study are described in the following subsections.

6.6.1 Direct Strain [CI/CD]

The direct strain method includes the calculation of circumferential, axial, and volumetric strain of a sample throughout the duration of testing. These three parameters are plotted together along the same axis and against axial stress. The trends observed in the data are analyzed to identify CI and CD thresholds (Figure 19).

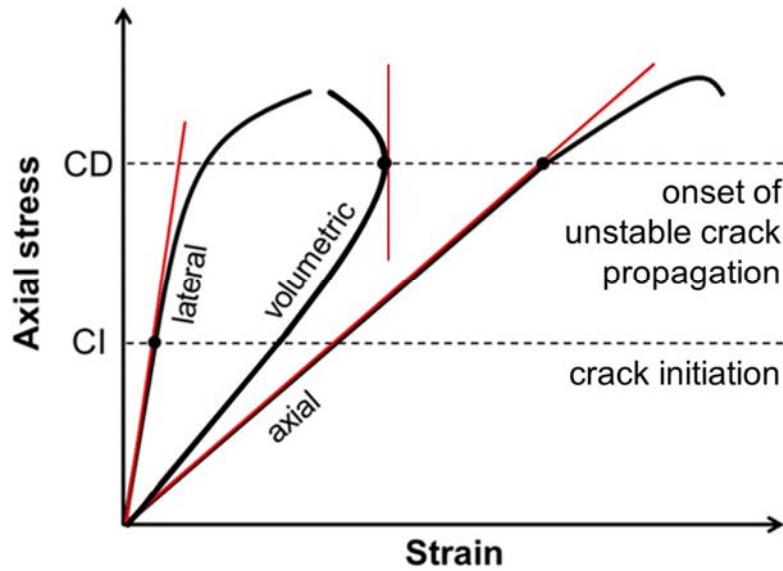


Figure 19: Example of strain-stress graph showing axial, lateral, and volumetric strain data and their associated CI and CD threshold markers

Circumferential (lateral) and axial strain is calculated according to the ASTM (2014) method, while volumetric strain is calculated using the ISRM (1979) guideline. CI is identified as the point of non-linearity in the slope of the direct circumferential strain data (Brace et al. 1966; Bieniawski 1967; Lajtai and Lajtai 1974). CD can be approximated as the point of non-linearity in the slope of the direct axial strain data, as well as the reversal point of volumetric strain.

6.6.2 Crack Volumetric Strain [ϵ_{cv}]

Crack volumetric strain (ϵ_{cv}) is an indicator that was suggested by Martin (1993) for determining the onset of CI threshold. This can be done by calculating the difference between volumetric strain (ϵ_{vol}) and elastic volumetric strain (ϵ_{ev}), as shown in Equation 6:

$$\epsilon_{cv} = \epsilon_{vol} - \epsilon_{ev} \quad [6]$$

in which volumetric strain is a function of axial (ϵ_{axial}) and lateral ($\epsilon_{lateral}$) strain. This relationship can be seen below in Equation 7:

$$\epsilon_{vol} = \epsilon_{axial} + 2 \epsilon_{lateral} \quad [7]$$

Elastic volumetric strain is given by Equation 8:

$$\epsilon_{ev} = \frac{1-2\nu}{E} (\sigma_1 - \sigma_3) \quad [8]$$

where E and ν are Young's modulus and Poisson's ratio respectively, and σ_1 and σ_3 are the major and minor principle stresses. The corresponding plot of stress and crack volumetric strain shows a gradual increase as pre-existing fractures within the specimen close. E35 and v35 should be used for this calculation. Eventually, the ϵ_{cv} trend flattens and begins to decrease rapidly. CI is interpreted as the maximum (reversal) point of the crack volumetric strain curve.

6.6.3 Inverse Tangent Lateral Stiffness (ITLS)

Ghazvinian (2010) suggests Inverse Tangent Lateral Stiffness (ITLS) as a CI estimation method that is only dependent on lateral strain. ITLS utilizes a moving point regression technique to amplify the change in slope of the lateral strain-axial stress curve. ITLS ($\varepsilon_1\Delta$) is calculated using Equations 9, 10, and 11:

$$\varepsilon_1\Delta = \frac{\Delta\varepsilon_{lateral}}{\Delta\sigma} \quad [9]$$

where,

$$\Delta\varepsilon_{lateral} = \varepsilon_{lateral\ i+10} - \varepsilon_{lateral\ i-10} \quad (i=1, 2, 3, \dots) \quad [10]$$

$$\Delta\sigma = \sigma_{i+10} - \sigma_{i-10} \quad (i=1, 2, 3, \dots) \quad [11]$$

and σ is the axial stress. Both $\Delta\varepsilon_1$ and $\Delta\sigma$ are calculated between an interval which is adjusted by the user according to data quality and data frequency to reduce noise (Ghazvinian 2015). In this method, CI is identified as the onset of non-linearity of the ITLS curve when plotted against axial stress.

6.6.4 Instantaneous Poisson's Ratio [$v\Delta$]

Instantaneous Poisson's Ratio ($v\Delta$) is a useful method for identifying the onset of CI using a moving point regression. This technique amplifies the change in Poisson's Ratio during testing, capturing the increase in lateral strain rate as fractures begin to form within the specimen (Diederichs 1999). The moving average of Poisson's Ratio is calculated using Equations 10, 12, and 13:

$$v\Delta = \frac{\Delta\varepsilon_{lateral}}{\Delta\varepsilon_{axial}} \quad [12]$$

where

$$\Delta\varepsilon_{axial} = \varepsilon_{axial\ i+10} - \varepsilon_{axial\ i-10} \quad (i=1, 2, 3, \dots) \quad [13]$$

and $\Delta\varepsilon_{lateral}$ is given in Equation 6. CI is identified as the onset of non-linearity of the $v\Delta$ curve when plotted against axial stress.

6.6.5 Instantaneous Young's Modulus [CD]

Instantaneous Young's Modulus is similar to the previous two methods; it uses a moving point regression to make the rapid increase of axial strain more apparent. This rapid increase in strain under constant, or slightly increasing, axial stress represents the CD threshold. Instantaneous Young's Modulus is calculated using Equations 11, 13, and 14 described by Ghazvinian (2010):

$$E\Delta = \frac{\Delta\sigma}{\Delta\varepsilon_{axial}} \quad [14]$$

Instantaneous Young's Modulus initially shows a steady increase as cracks within the specimen close, leading to a maximum value in the stress and $E\Delta$ plot. After this point the specimen will begin to behave as a linear elastic material. This behaviour will continue to be captured in the $E\Delta$ plot even after new cracks parallel to the direction of loading form. Once

the fracture density within the sample is large enough to cause interaction between one another the $E\Delta$ slope will begin to decrease significantly indicating the CD threshold.

6.6.6 Acoustic Emission (AE) Methods [CI/CD]

Diederichs et al. (2004) describes an AE method for identification of CI and CD thresholds using a plot of cumulative number of AE events against axial stress. A lower bound for CI is identified as the point where the rate of AE events begins to occur at an increased rate with little change in axial stress. The upper bound for CI is identified as the second point of increase in the rate of AE events. The rate of AE events will begin to rapidly increase at this point, before eventually becoming linear. The final rapid increase in the rate of AE events before failure of the sample represents the CD threshold. A mid-bound value (CI_M) is also identified, representing the intersection of the trendlines for AE data after first cracking (CI_L) and after systematic damage (CI_U).

7. RESULTS

The previously described testing has produced stress, strain, and AE data for 54 Uniaxial Compressive Strength (UCS) and 47 Brazilian Tensile Strength (BTS) Cobourg limestone specimens. A data summary of the UCS and BTS results is included in Appendix 5 and 6, respectively. This data has been used to calculate UCS, axial strain, circumferential (lateral) strain, Poisson's ratio, and Young's modulus using the ASTM 7012 (2014) standard methods. It has also been used to calculate BTS in accordance with ASTM D3967 (2008b). Water content (%) for all specimens has been calculated using the ASTM (2010) standard method. In addition, CI and CD thresholds are calculated as an average of several indicator methods previously described. The results of the testing program have been categorized first by test type and then by testing condition.

7.1 Uniaxial Compressive Strength (UCS) Results

A total of 54 UCS specimens of Cobourg limestone were prepared and tested under various conditions to investigate the influence of saturation, scale, and loading rate on the geomechanical properties of the rock. In total, 18 specimens were used to evaluate the influence of saturation, 12 specimens were used to evaluate the influence of scale, and 24 specimens were used to evaluate the influence of loading rate.

7.1.1 Saturation

The water content of specimens used to investigate the influence of saturation was varied using the seven methods previously discussed in Section 4.5 of this report. All specimens consisted of cylindrical samples of Cobourg limestone, with a diameter of 76 mm. The same dimensions were used for the three 76 mm specimens used to investigate the influence of scale, thus they have been included within this data set for comparison. The three scale specimens remained exposed to Room Relative Humidity (RRH) while being stored within the preparation laboratory, and will represent a seventh saturation state for the subsequent data. Therefore, these results will include a total of 21 data points from seven different saturation methods.

7.1.1.1 Water Content

The water content (%) of the specimens has been calculated and compared to the various saturation methods used. The data is shown below in Figure 20.

The oven drying methods have shown a significant decrease in water content of the specimens. The one month drying produced an average water content of 0.05%, while the two week oven drying had an average of 0.08%. The RRH specimens had variable water contents ranging from 0.18% to 0.32%. The saturated specimens all resulted in similar water contents with the one-week vacuum saturation, one-week submersion, and one-month submersion specimens having an average water content of 0.606%, 0.610%, and 0.612%, respectively. The average water content of the three-month submersion saturated specimens was slightly higher at 0.651%. The minimum, maximum, and average water content of the specimens has been summarized in Table 7.

It was noted that long durations of unconfined saturation by immersion resulted in some visible sample damage where locally concentrated clay matrix was present. Under in situ situation, damage is not anticipated during re-saturation of rock underground. It is important to note that some differences in testing results for three-month samples may be the result of this damage rather than the direct result of increased saturation times.

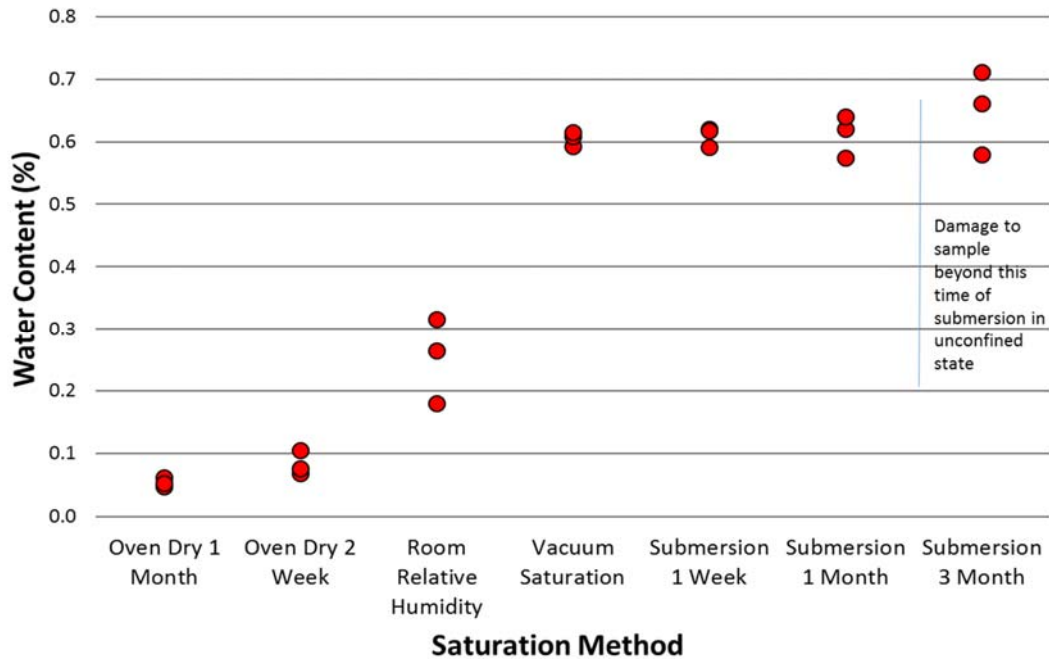


Figure 20: Comparison of water content and saturation method for UCS specimens

Table 7: Summary of water content results

Saturation Condition	Water Content %		
	Min.	Max.	Avg.
Oven Dry 1 Month	0.05	0.06	0.054
Oven Dry 2 Week	0.07	0.11	0.083
Room Relative Humidity	0.18	0.32	0.254
Vacuum Saturation	0.59	0.62	0.606
Submersion 1 Week	0.59	0.62	0.610
Submersion 1 Month	0.57	0.64	0.612
Submersion 3 Month	0.58	0.71	0.651

7.1.1.2 Elastic Properties

Poisson's ratio and Young's modulus have been calculated for all specimens using the previously discussed methods. A comparison of the calculated Poisson's ratio and Young's modulus, with respect to water content, can be seen below in Figure 21.

The comparison shows a slight increasing trend in Poisson's ratio and decreasing trend in Young's modulus with increasing water content. There is also increased variability in both Young's modulus and Poisson's ratio values for the saturated specimens. The trends appear to level out at the higher water contents, approaching constant values for both Young's modulus and Poisson's ratio. Data regarding minimum, maximum, and average Young's modulus and Poisson's ratio is shown in Table 8.

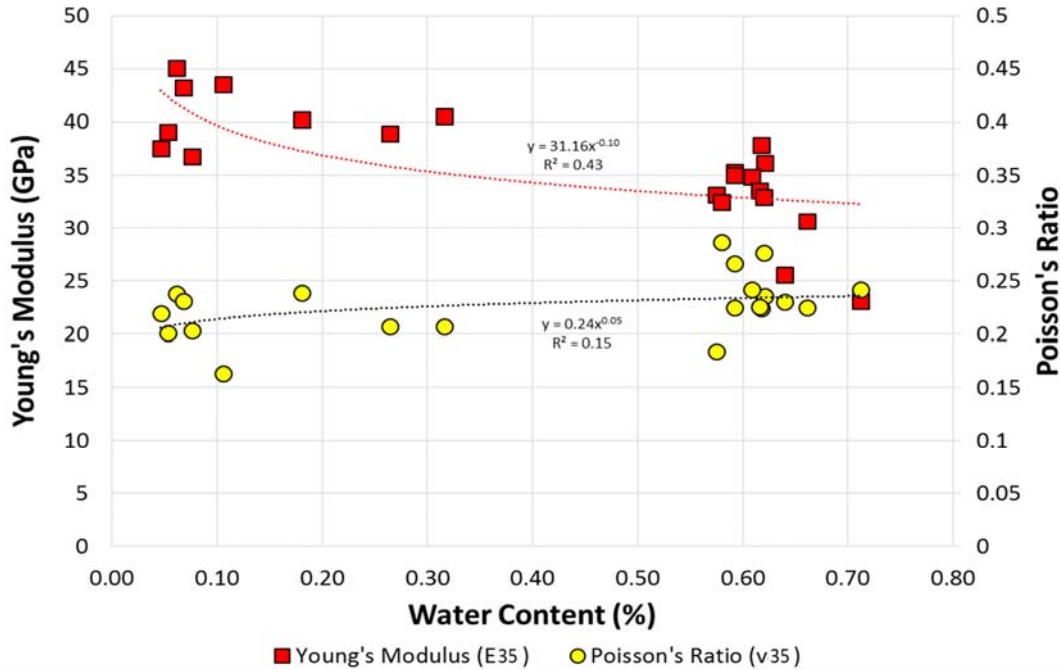


Figure 21: Poisson's ratio and Young's modulus (GPa) compared to the water content

Table 8: Young's modulus (E35) and Poisson's Ratio (v35) data for saturation specimens.

Saturation Condition	Young's Modulus (GPa)			Poisson's Ratio		
	Min.	Max.	Avg.	Min.	Max.	Avg.
Oven Dry 1 Month	38	45	40.5	0.20	0.24	0.219
Oven Dry 2 Week	37	44	41.2	0.16	0.23	0.199
Room Relative Humidity	39	40	39.9	0.21	0.24	0.217
Vacuum Saturation	34	35	34.4	0.22	0.24	0.231
Submersion 1 Week	35	38	36.4	0.22	0.27	0.242
Submersion 1 Month	26	33	30.5	0.18	0.28	0.230
Submersion 3 Month	23	32	28.7	0.22	0.29	0.251

Although the vacuum, one week, one-month, and three-month saturated specimens all have similar water contents, they produce significantly different results with respect to elastic properties. The data in Table 8 shows that as saturation duration increases, there is a decrease in Young's modulus and increase in Poisson's ratio. The two week and one-month oven-dried specimens, as well as RRH specimens, produced relatively similar results with respect to elastic constants. This suggests that increased oven drying duration would not influence Young's modulus or Poisson's ratio in a significant manner.

7.1.1.3 UCS and Crack Damage Thresholds

The CI and CD thresholds have been estimated using a variety of methods based on the stress, strain, and AE data obtained during testing. These methods have been previously discussed in subsection 6.6. In addition, UCS has been calculated based on the peak load measured during each test. These strength thresholds have been plotted together with respect to water content of the specimens in Figure 22.

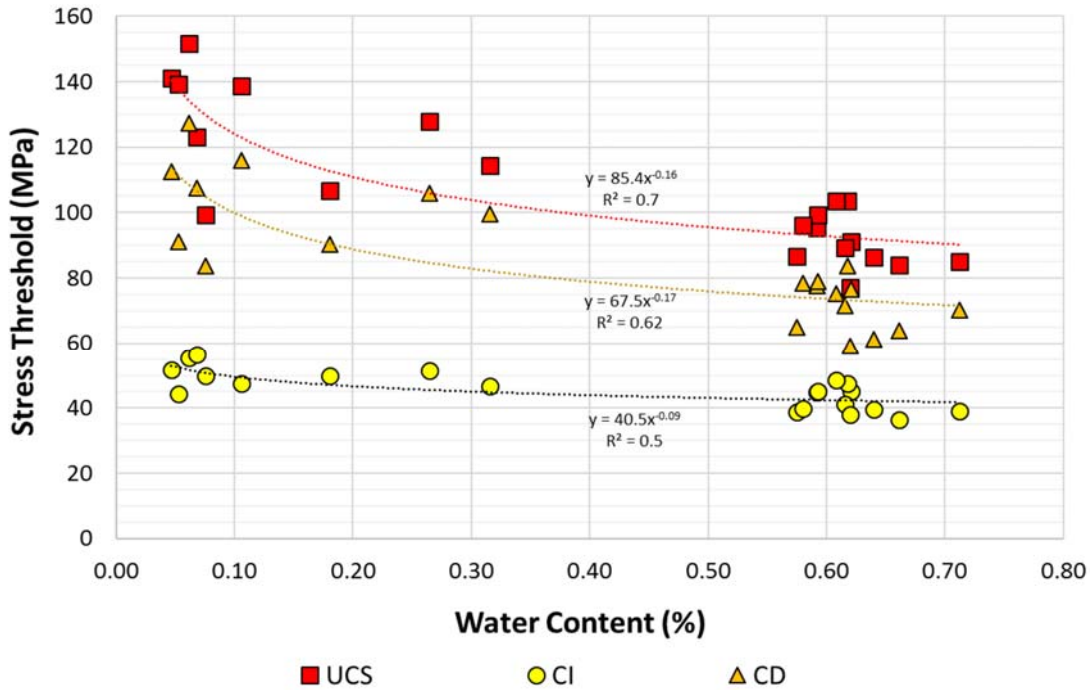


Figure 22: Comparison of CI, CD, and UCS stress thresholds with respect to specimen water content

Figure 23 shows that with increasing water content there is a significant decrease in both UCS and CD. The influence of increasing water content on the CI threshold of Cobourg limestone appears to be minor, and approaching a constant value at higher saturation. The one-month oven-dried specimens produced a maximum and minimum UCS of 151.8 MPa and 139.1 MPa respectively, a range of 12.7 MPa. The three-month submersion saturated specimens produced a maximum UCS of 96.2 MPa and a minimum UCS of 84.0 MPa, a range of 12.2 MPa. The drop in average UCS from fully dry (one-month oven drying) to fully saturated (three-month submersion) is approximately 55.56 MPa, a decrease of 39%. The oven-dried, RRH, and saturated results have been grouped together and are summarized in Table 9.

Table 9: Thresholds from Best Fit Trends for dried, RRH, and saturated specimens

Threshold	Dried @0.065%	RRH @0.25%	Wet @0.65%	Increase from RRH-Dry (%)	Decrease from RRH-Wet (%)
CI	51.8	45.9	42.1	12.9	8.2
CD	107.4	85.4	72.6	25.7	15.0
UCS	132.2	106.6	91.5	24.0	14.2

The data in Table 9 supports a general decreasing trend in UCS and crack damage thresholds, however, with a noticeably smaller effect on CI. The reverse trend is shown with the oven-dried specimens, with minor influence on CI (12.9% increase), and more effect on CD (25.7% increase) and UCS (24.0% increase). Results for the seven individual saturation conditions are summarized in Table 10.

Table 10: UCS and crack damage threshold data for saturation specimens

Saturation Condition (Number of Tests)	CI (MPa)			CD (MPa)			UCS (MPa)		
	Min.	Max.	Avg.	Min.	Max.	Avg.	Min.	Max.	Avg.
Oven Dry 1 Month (3)	44.3	55.4	50.48	91.0	127.3	110.25	139.1	151.8	143.95
Oven Dry 2 Week (3)	47.5	56.4	51.23	83.7	116.0	102.39	99.3	138.7	120.35
Room Relative Humidity (3)	46.7	51.5	49.33	90.3	106.0	98.58	106.8	127.9	116.32
Vacuum Saturation (3)	41.3	48.6	45.02	71.5	79.0	75.28	89.2	103.4	97.34
Submersion 1 Week (3)	44.8	47.5	45.78	76.7	83.8	79.39	91.2	103.6	96.72
Submersion 1 Month (3)	38.1	39.6	38.82	59.3	65.0	61.83	77.2	86.7	83.44
Submersion 3 Month (3)	36.3	39.8	38.37	64.0	78.5	70.92	84.0	96.2	88.39

The range in average CI between all saturation methods is 13 MPa, much less than the ranges produced by average CD and UCS which are 48 MPa and 61 MPa respectively. The oven-dried and RRH specimens all produced similar average CI thresholds. The CD and UCS results for the same group of specimens varied more, with the two-week oven-dried and RRH specimens having the most similar results. The vacuum and one-week submersion saturated specimens produced very similar CI, CD, and UCS results. The one-month and three-month saturated specimens behaved very similarly with respect to CI. These results show that saturation duration has a more marked influence on CI in comparison to the grouped results shown in Table 9.

The three-month saturated specimens produced an average CI of 38.37 MPa, approximately 22% less than the average RRH results (49.33 MPa). This decrease is more significant than that observed between RRH and average saturated results (Table 9), however, this may not be an accurate representation of the influence of pore water pressure. The one and three-month saturated specimens also produced noticeably lower CI values in comparison to one-week and vacuum saturated specimens with comparable water contents. This suggests that the observed decrease in one and three-month saturated specimens is not a direct influence of pore pressure, but rather a more complex mechanism involving interaction of specimens with the SPW fluid used for saturation. The grouped results (Table 9) may be more representative of the general influence of re-saturation on the Cobourg limestone.

All CI and CD thresholds represent an average of the six previously discussed estimation methods, used to represent a single identifiable value for each specimen. In addition to the variability of average CI thresholds mentioned above, there is significant variability between the results of the individual CI indicators used within these averages. To further investigate this variability, the five CI indicators used to calculate CI threshold have been plotted against water content in Figure 23.

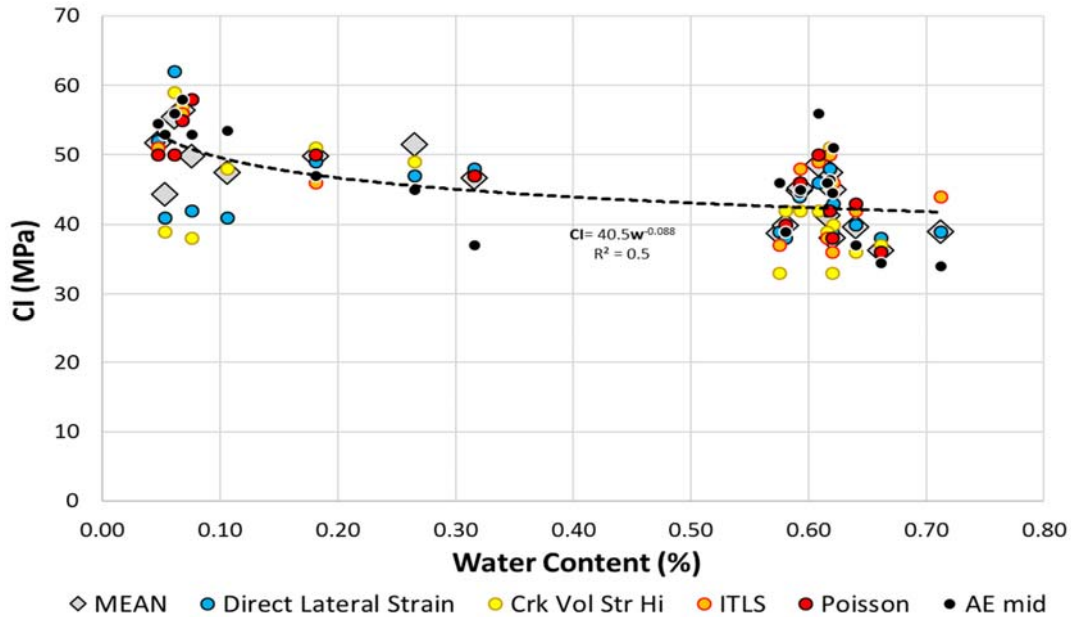


Figure 23: Crack Initiation (CI) indicator for saturation specimens based on six different methods: direct lateral strain, crack volumetric strain, inverse tangent lateral stiffness, instantaneous Poisson's ratio, acoustic emissions, and mean values from all methods

The mean value, representing the CI thresholds presented in Figure 22, has also been included for reference. The plot shows the same decreasing trend observed for the CI thresholds, however, with much more variability between the individual CI indicators. In addition, values for some of the estimation methods may have unidentifiable based on the specified technique and test data obtained. Due to this, some of the mean values do not include all five CI indicators.

7.1.2 Scale

The influence of scale on the elastic and strength properties of the Cobourg limestone has been investigated through the testing UCS specimens with varying diameter. Three specimens have been prepared for each of the four diameters. The four diameters investigated in this study are 50 mm (2"), 76 mm (3"), 101 mm (4"), and 126 mm (5"). Each of the specimens has been prepared with a length to diameter ratio of 2.5. The loading rate of the specimens has been scaled up according to Table 6, to ensure a consistent axial strain rate throughout the tests. The following subsections will present the data for the 12 scale UCS tests.

7.1.2.1 Elastic Properties

The elastic properties of the scale tests have been calculated in accordance with ASTM D7012 (2014) standard. Young's modulus and Poisson's ratio have been plotted together in Figure 24 to assess the influence of changing scale.

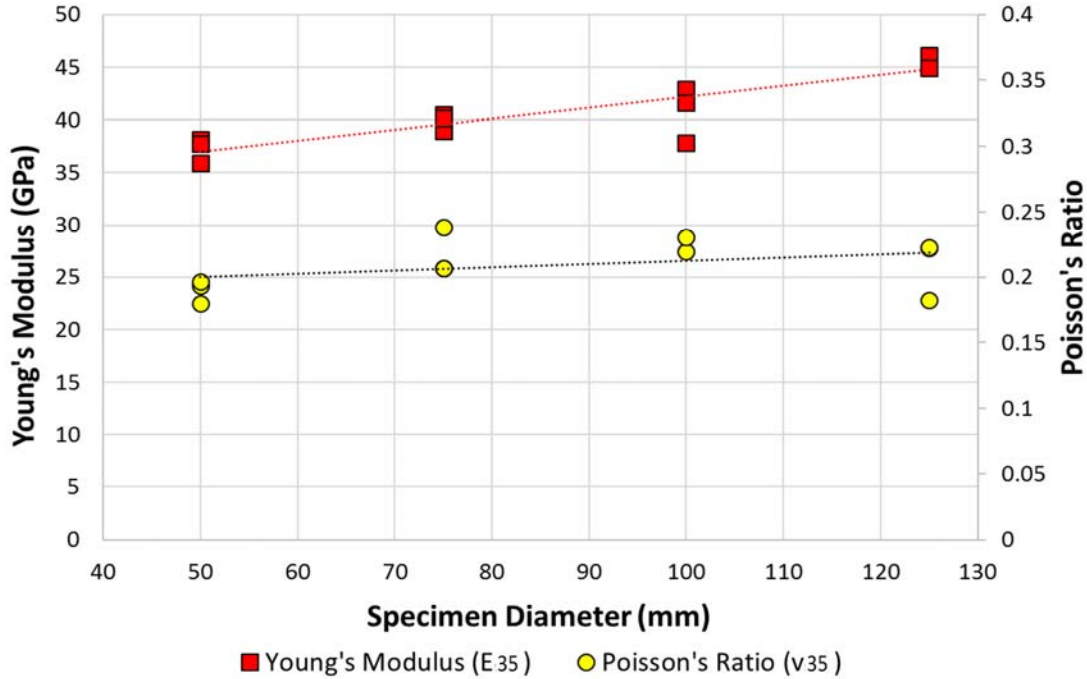


Figure 24: Poisson's ratio and Young's modulus compared to specimen diameter

The results show that there is a slight increasing trend in Young's modulus with increasing specimen diameter. This increasing trend could be associated with the larger specimens incorporating more intact portions of the structure inherent within the Cobourg limestone (i.e. large calcite rich nodules). This structure is dispersed throughout the smallest diameter samples but is incorporated more as specimen diameter increases. The calcite rich nodules present within the rock may begin to influence the stiffness of the specimen as it approaches a diameter which incorporates the structure in its entirety.

There is no significant effect on Poisson's ratio with increasing scale; the ratios of the specimens increase slightly for the 76 and 101 mm specimens and then drop at the largest diameter. There is increased variability in the Young's modulus results of the 101 mm diameter specimens, as well as Poisson's ratio of the 76 mm specimens. In general, the remaining data points are very similar for each specimen diameter. Data regarding minimum, maximum, and average Young's modulus and Poisson's ratio is shown in Table 11.

Table 11: Young's modulus (E35) and Poisson's ratio (v35) for scale specimens.

Specimen Diameter (mm)	Young's Modulus (GPa)			Poisson's Ratio		
	Min.	Max.	Avg.	Min.	Max.	Avg.
50	36	38	37.3	0.18	0.20	0.190
76	39	40	39.9	0.21	0.24	0.217
101	38	43	40.8	0.22	0.39	0.281
126	45	46	45.6	0.18	0.22	0.209

7.1.2.2 UCS and Crack Damage Thresholds

The obtained test data has been used to calculate UCS, CI, and CD stress thresholds. To investigate the influence of scale, these thresholds have been plotted against specimen diameter in Figure 25.

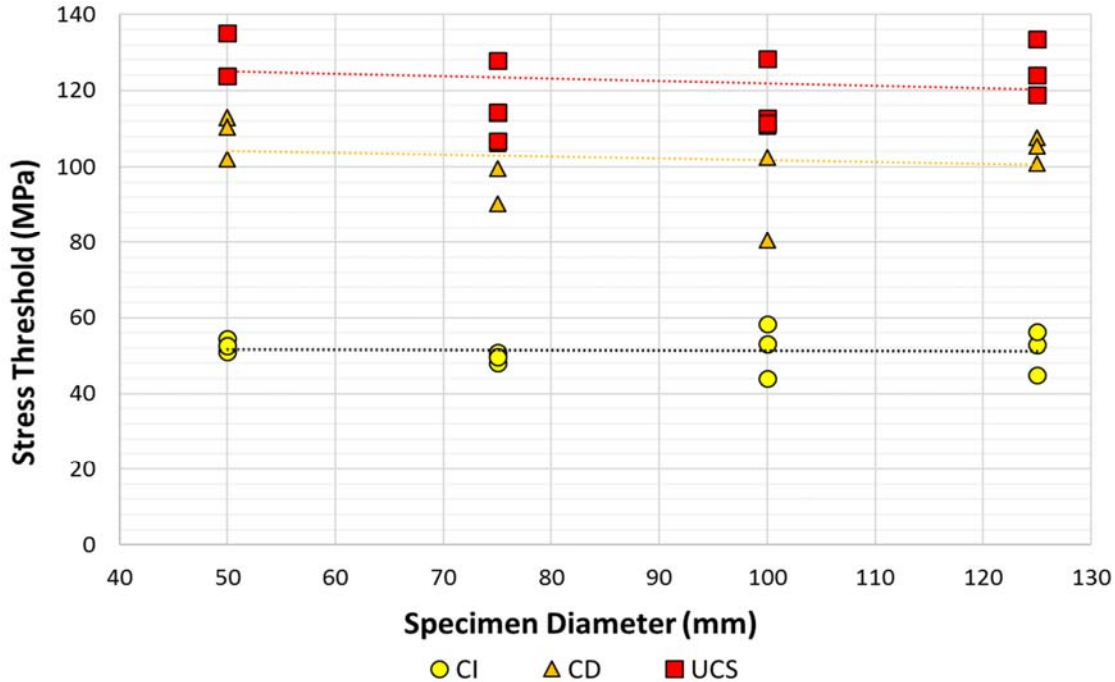


Figure 25: Comparison of CI, CD, and UCS stress thresholds with respect to specimen diameter

The results show that there is a minor decrease in UCS and CD for the 76 and 101 mm specimens with respect to the 50 and 126 mm specimens. The CI trend of these tests remains constant, at approximately 51 MPa. This suggests that changing scale has a negligible influence on these thresholds. The data from the scale tests has been summarize in Table 12. The CI data shows that there is greater variability for the 101 and 126 mm tests. This trend does not exist for CD and UCS results, which are more variable in general for all four specimen diameters.

Table 12: UCS and crack damage threshold data for scale specimens

Specimen Diameter (mm)	CI (MPa)			CD (MPa)			UCS (MPa)		
	Min.	Max.	Avg.	Min.	Max.	Avg.	Min.	Max.	Avg.
50	51.1	54.4	52.72	102.0	113.0	108.43	123.8	135.0	131.27
76	48.0	50.8	49.48	90.3	106.0	98.58	106.8	127.9	116.32
101	44.0	58.3	51.80	80.5	110.7	97.89	111.3	128.4	117.44
126	45.0	56.3	51.35	101.0	107.7	104.67	118.9	133.6	125.51

The five individual CI indicators used to calculate CI threshold have been plotted against specimen diameter in Figure 26 to investigate the influence of specimen scale. The mean value, representing the CI thresholds presented in Figure 25, has also been included for reference. The plot shows the same trend observed for the CI thresholds, maintaining a relatively constant range of values between 45 and 60 MPa. The range of individual CI

indicators for the 50 and 76 mm specimens are quite similar. The variation in indicators is greater for the 126 mm specimens and the largest in the 101 mm results, supporting the results observed with CI threshold in Figure 25. There is an increased likelihood for larger diameter specimens to have imperfections and pre-existing fractures present, which is believed to influence the UCS of most rock types (Hoek and Brown, 1980). While there is no clear indication that the increased chance of imperfections and pre-existing fractures influences CI, this could be one of the factors influencing the variability of CI indicators for the larger specimen diameters.

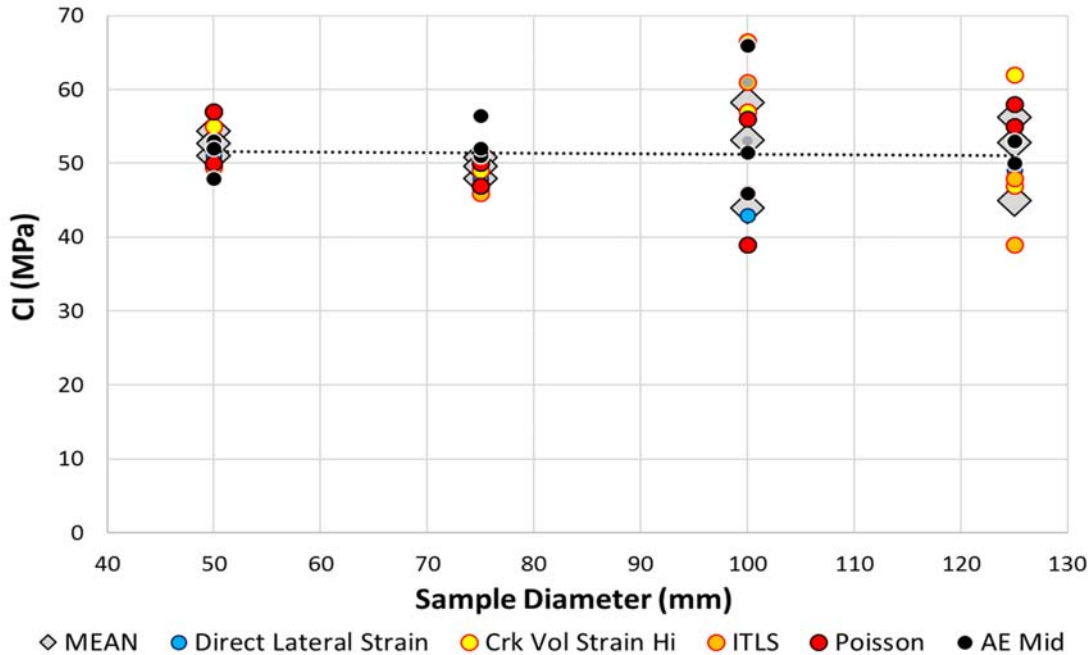


Figure 26: Crack Initiation (CI) indicator for scale specimens based on six different methods: direct lateral strain, crack volumetric strain, inverse tangent lateral stiffness, instantaneous Poisson's ratio, acoustic emissions, and mean values from all methods

7.1.3 Loading Rate

The effect of loading rate on the geomechanical properties of the Cobourg limestone has been investigated for both Room Relative Humidity (RRH) and one-month saturated specimens having a consistent diameter of 76 mm. Specimens have been tested at four target failure times in groups of three. These target times are 2, 6, 60, and 600 minutes and are adapted from the standard loading rates used for 20 minute saturation and scale testing. The previously presented saturation results include 76 mm specimens with RRH and one-month submersion saturation conditions and can be used for loading rate comparison as well. These saturation results will be represented with target failure times of 20 minutes and will be presented as the 5th loading rate set for both saturation conditions. The target failure times used have been summarized in Table 13 below, including the axial deformation, circumferential deformation, and axial strain rate used in each case. The following subsections will present the results of 30 UCS tests on RRH and one-month saturated loading rate specimens.

Table 13: Summary of deformation and strain rates used to achieve targeted failure times

Target Failure Time (min)	Axial Deformation Rate (mm/min)	Circumferential Deformation Rate (mm/min)	Axial Strain Rate Equivalent ($\mu\epsilon/\text{min}$)
2	0.1000	0.125000	2000
6	0.0300	0.037500	600
20	0.0100	0.012500	200
60	0.0030	0.003750	60
600	0.0003	0.000375	6

7.1.4 Room Relative Humidity (RRH) Results

7.1.4.1.1 Elastic Properties

To assess the influence of loading rate on the elastic properties of Cobourg limestone, the calculated Young's modulus and Poisson's ratio have been plotted together with respect to axial strain rate (Figure 27).

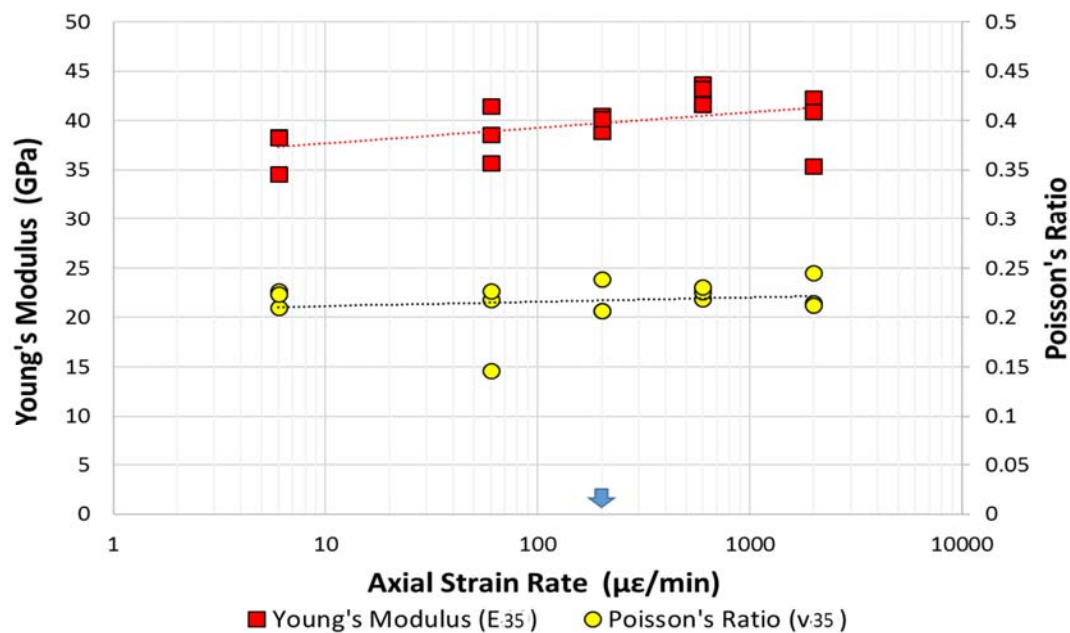


Figure 27: Poisson's ratio and Young's modulus vs axial strain rate for RRH. The blue arrow represents the standard axial strain rate used for saturation and scale tests

This comparison shows that with increasing axial strain rate there is a gradual increase in Young's modulus with no significant effect on Poisson's ratio. The 60 minute specimens represent the most variable data for Poisson's ratio, while also showing increased variability for Young's modulus. The 2 minute specimens also show increased variability for Young's modulus. In general, the remaining data points have similar results within the same targeted failure time. Data for minimum, maximum, and average Young's modulus and Poisson's ratio has been included in Table 14. This data highlights the variability of the 60 and 2 minute failure time tests. While the data presented in Figure 27 suggests a minor increasing trend, the average Young's modulus calculated for the 2 and 600 minute tests are similar. The

same is true for average Poisson's ratio, supporting a more constant Young's modulus and Poisson's ratio trend across all five of the targeted failure times.

Table 14: Young's modulus (E35) and Poisson's ratio (v35) data for RRH loading rate specimens.

Target Failure Time (min)	Axial Strain Rate ($\mu\epsilon/\text{min}$)	Young's Modulus (GPa)			Poisson's Ratio		
		Min.	Max.	Avg.	Min.	Max.	Avg.
2	2000	35	42	39.5	0.21	0.24	0.224
6	600	42	44	42.8	0.22	0.23	0.225
20	200	39	40	39.9	0.21	0.24	0.217
60	60	36	41	38.6	0.15	0.23	0.197
600	6	35	38	37.0	0.21	0.23	0.220

7.1.4.1.2 UCS and Crack Damage Thresholds

To investigate the influence of loading rate on CI, CD, and UCS of RRH specimens, these thresholds have been plotted against axial strain rate (Figure 28).

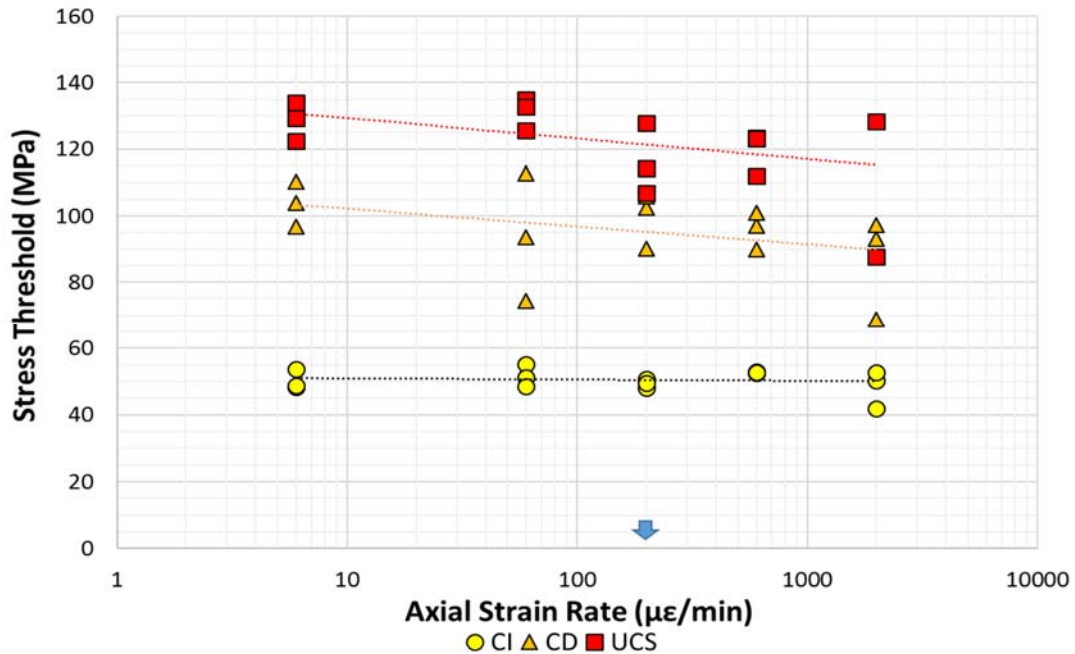


Figure 28: Comparison of CI, CD, and UCS stress thresholds with respect to axial strain rate for RRH specimens. The blue arrow represents the standard axial strain rate used for saturation and scale tests.

The strength and crack damage threshold data suggest a decreasing trend for CD and UCS with respect to increasing axial strain rate. Similar to the elastic properties, there is increased variability in the CD results of the 60 minute failure time tests. In addition, the CD and UCS results of the 2 minute tests are also quite variable, ranging from 68.8 to 97.3 MPa for CD and 87.8 to 128.3 MPa for UCS. Results from the remaining target failure times are similar within the same group, and the CI results remain relatively constant for all target times. The minimum, maximum, and average CI, CD, and UCS results have been summarized in Table 15.

Table 15: UCS and crack damage threshold data for RRH loading rate specimens

Target Failure Time (min)	Axial Strain Rate ($\mu\epsilon/\text{min}$)	CI (MPa)			CD (MPa)			UCS (MPa)		
		Min.	Max.	Avg.	Min.	Max.	Avg.	Min.	Max.	Avg.
2	2000	42.0	52.7	48.33	68.8	97.3	86.36	87.8	128.3	114.81
6	600	52.6	53.0	52.78	90.0	101.0	96.00	112.0	123.5	119.49
20	200	48.0	50.8	49.48	90.3	106.0	99.58	106.8	127.9	116.32
60	60	48.5	55.2	51.62	74.5	112.7	93.61	125.5	135.0	131.10
600	6	48.4	53.7	50.29	96.7	110.3	103.65	122.5	133.9	128.57

Average CI threshold varies between 48.33 and 52.78 MPa across all five of the target failure times, with the largest variability between specimens occurring for the 2 minute target time. Due to the variability of the 60 minute CD results, the minimum and average values for that target time are slightly lower than the expected trend in the data. Excluding the 2 minute results, the UCS data is consistent within each target time and supports a decreasing trend with increasing axial strain rate. The individual CI indicators have been plotted against axial strain rate to evaluate the variability between indicators (Figure 29).

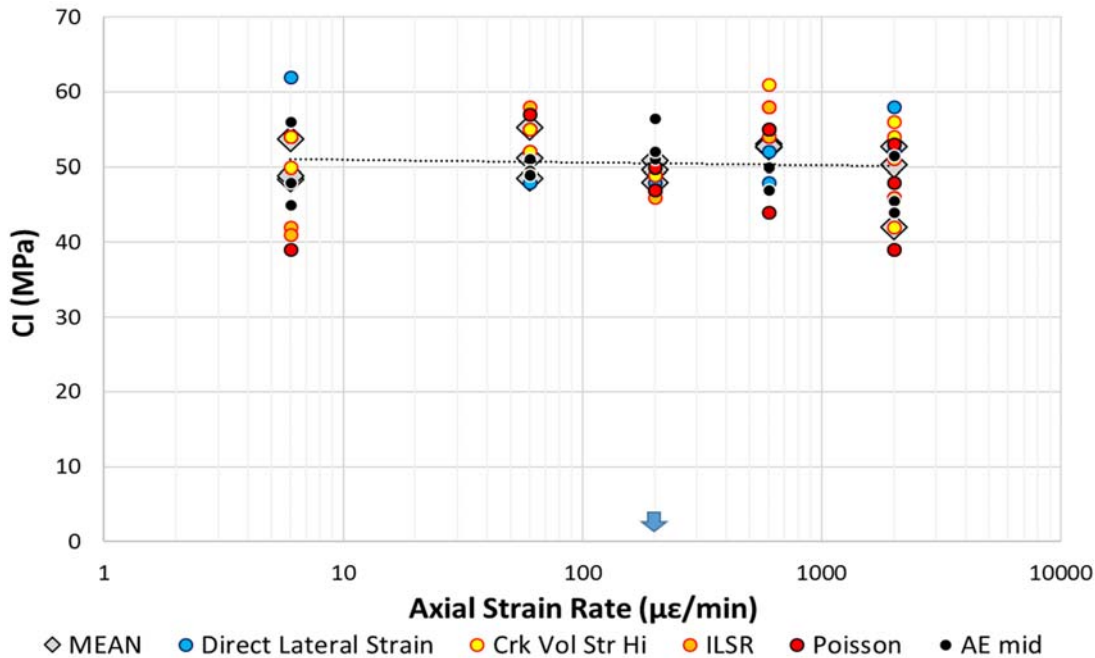


Figure 29: Crack Initiation (CI) indicator for RRH specimens based on six different methods: direct lateral strain, crack volumetric strain, inverse tangent lateral stiffness, instantaneous Poisson's ratio, acoustic emissions, and mean values from all methods. The blue arrow represents the standard axial strain rate.

The plot shows the same plateau trend observed for the CI thresholds in Figure 28, maintaining a relatively constant trend. Almost all of the individual CI indicators for all five target failure times fall within the 40 to 60 MPa range, with most resulting in similar values for a given strain rate.

7.1.4.2 One-month Saturated Results

7.1.4.2.1 Elastic Properties

A plot has been created with elastic property data and axial strain rates to compare the influence of loading rate on Young's modulus and Poisson's ratio of one-month saturated specimens (Figure 30).

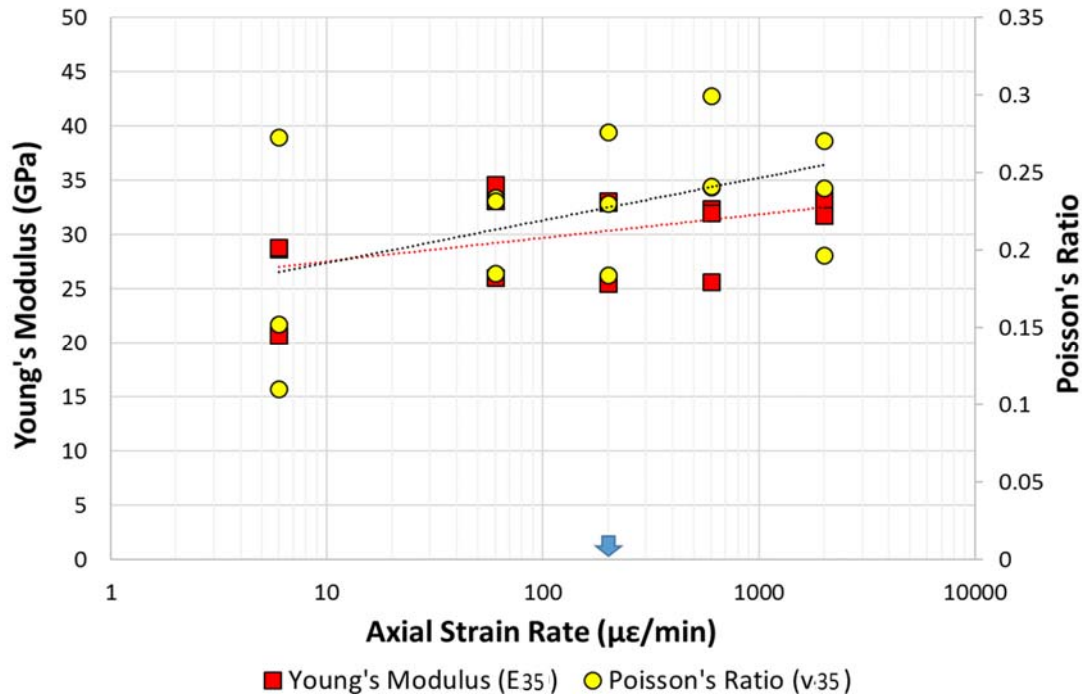


Figure 30: Poisson's ratio and Young's modulus compared to the axial strain rate for one-month saturated specimens. The blue arrow represents the standard axial strain rate used for saturation and scale tests

The results of the one-month saturated specimens show that there is a minor increasing trend for both Young's modulus and Poisson's ratio with increasing axial strain. The trend of the Young's modulus data is very similar to that observed in Figure 27, although the values are much lower. The large range between some of the data points makes it difficult to propose a definite relationship for Young's modulus. Increased variability is also present in the Poisson's ratio data. The minimum, maximum, and average Young's modulus and Poisson's ratio values have been summarized in Table 16. It should be noted that the 600 minute tests result have the lowest minimum Young's modulus (21 GPa) and Poisson's ratio (0.11) throughout the entire testing program. Excluding the 600 minute test results, the average Young's modulus values for the remaining tests are relatively consistent and range between 30.0 to 32.7 GPa. Average Poisson's ratio behaves relatively consistent as well, ranging between 0.217 and 0.261 for the 2, 6, 20, and 60 minute tests.

Table 16: Young's modulus (E35) and Poisson's ratio (v35) data for one-month saturated loading rate specimens.

Target Failure Time (min)	Axial Strain Rate ($\mu\epsilon/\text{min}$)	Young's Modulus (GPa)			Poisson's Ratio		
		Min.	Max.	Avg.	Min.	Max.	Avg.
2	2000	32	33	32.7	0.20	0.27	0.236
6	600	26	32	30.0	0.24	0.30	0.261
20	200	26	33	30.5	0.18	0.28	0.230
60	60	26	35	31.3	0.19	0.23	0.217
600	6	21	29	26.1	0.11	0.27	0.179

7.1.4.2.2 UCS and Crack Damage Thresholds

To investigate the influence of loading rate on CI, CD, and UCS of one-month saturated specimens, the thresholds have been plotted against axial strain rate (Figure 31).

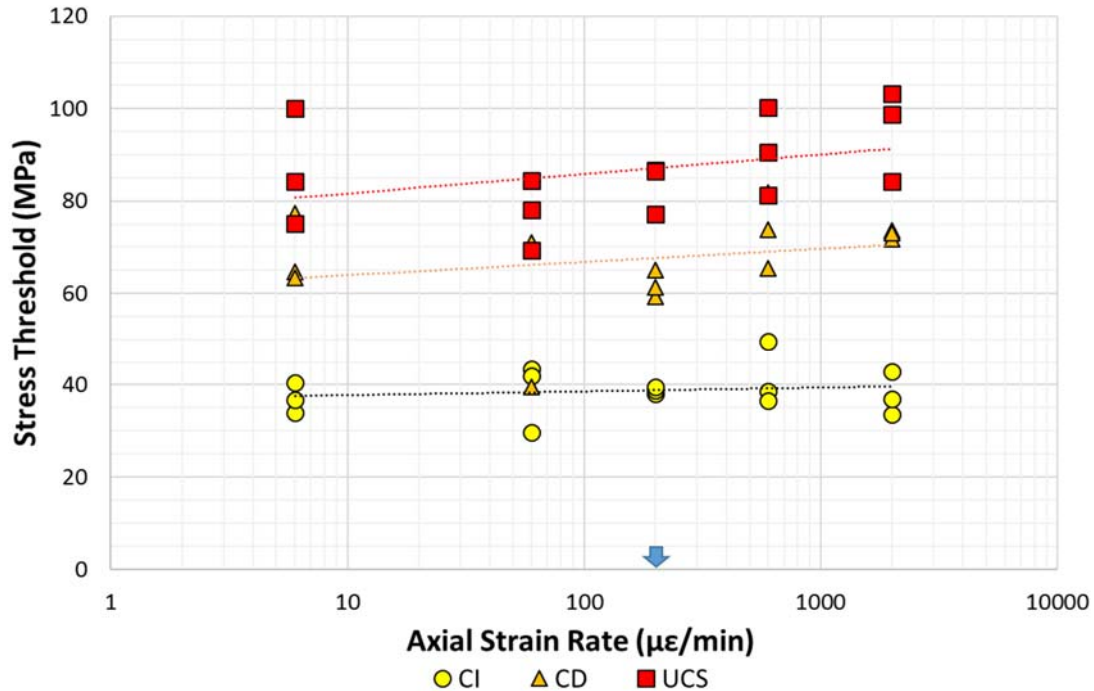


Figure 31: Comparison of CI, CD, and UCS stress thresholds with respect to axial strain rate for one-month saturated specimens. The blue arrow represents the standard axial strain rate used for saturation and scale tests

The above data shows a slightly increasing trend for CD and UCS with respect to increasing axial strain rate. This is an opposite trend that is observed in Figure 28 for the RRH specimens. The CI threshold results are relatively constant with increasing axial strain rate, suggesting no influence on CI. The minimum, maximum, and average CI, CD, and UCS results are summarized in Table 18.

Table 17: UCS and crack damage threshold data for one-month saturated loading rate specimens

Target Failure Time (min)	Axial Strain Rate ($\mu\epsilon/\text{min}$)	CI (MPa)			CD (MPa)			UCS (MPa)		
		Min.	Max.	Avg.	Min.	Max.	Avg.	Min.	Max.	Avg.
2	2000	33.6	42.9	37.83	71.8	73.7	72.81	84.2	103.2	95.33
6	600	36.6	49.5	41.58	65.5	81.8	73.67	81.2	100.3	90.71
20	200	38.1	39.6	38.82	59.3	65.0	61.83	77.2	86.7	83.44
60	60	29.6	43.5	38.37	39.5	71.0	59.94	69.3	84.5	77.27
600	6	34.0	40.5	37.10	63.3	77.3	68.44	75.1	100.0	86.45

The data in Table 17 shows that there is a significant decrease in average CD and UCS for both the 20 and 60 minute one-month saturated specimens with respect to the remaining tests. This decrease is not observed for average CI, which stays within the range of 37.10 to 41.58 MPa for all five target times. The two lowest CI averages were produced by the 2 and 600 minute tests; the two ends of the target failure time range. This supports the trend observed in Figure 31, suggesting that loading rate has no significant influence on CI threshold.

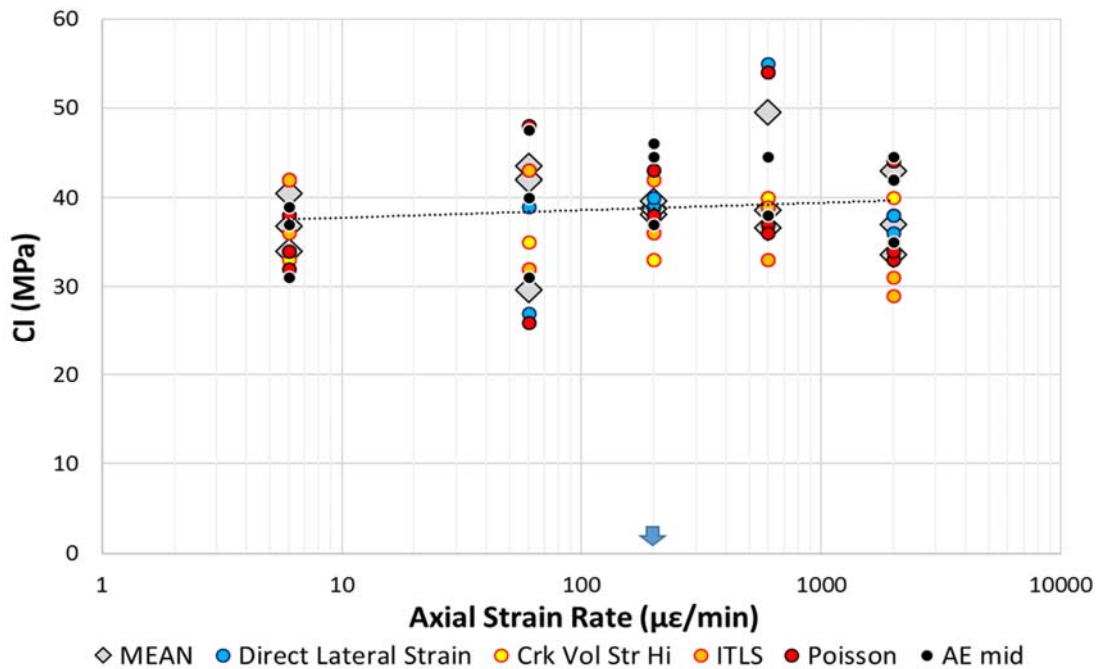


Figure 32: Crack Initiation (CI) indicator for one-month saturated specimens based on six different methods: direct lateral strain, crack volumetric strain, inverse tangent lateral stiffness, instantaneous Poisson's ratio, acoustic emissions, and mean values from all methods. The blue arrow represents the standard axial strain rate used for saturation and scale tests

Individual CI indicators have been plotted against axial strain rate to evaluate the variability associated with these estimation methods (Figure 32). The plot shows the same flat trend observed for the CI thresholds in Figure 31. The variability in individual CI indicators appears

to be slightly larger for the one-month saturated specimens in comparison to the RRH specimens, with values ranging between 26 to 55 MPa. This is especially true for the 6 and 60 minute failure time tests.

7.2 Brazilian Tensile Strength (BTS) Results

A total of 47 Cobourg limestone specimens were prepared and tested under various conditions to investigate the influence of saturation and scale on the BTS of the rock. In total, 30 specimens were used to evaluate the influence of saturation and 17 specimens were used to evaluate the influence of scale.

7.2.1 Saturation

The water content of 30 BTS specimens has been varied using six methods previously discussed in Section 4.5 this report. The specimens are Brazilian discs prepared from 76 mm drill core with a thickness to diameter ratio of 0.5. These dimensions match the three 76 mm specimens used to evaluate the influence of scale. These three specimens will be included in the saturation data set and will serve as a seventh saturation condition for further comparison. The results below will, therefore, represent the data from 33 BTS tests prepared with seven different saturation methods.

7.2.1.1 Water Content

The water content of the specimens has been calculated and compared to the various saturation methods used. The data is shown below in Figure 33.

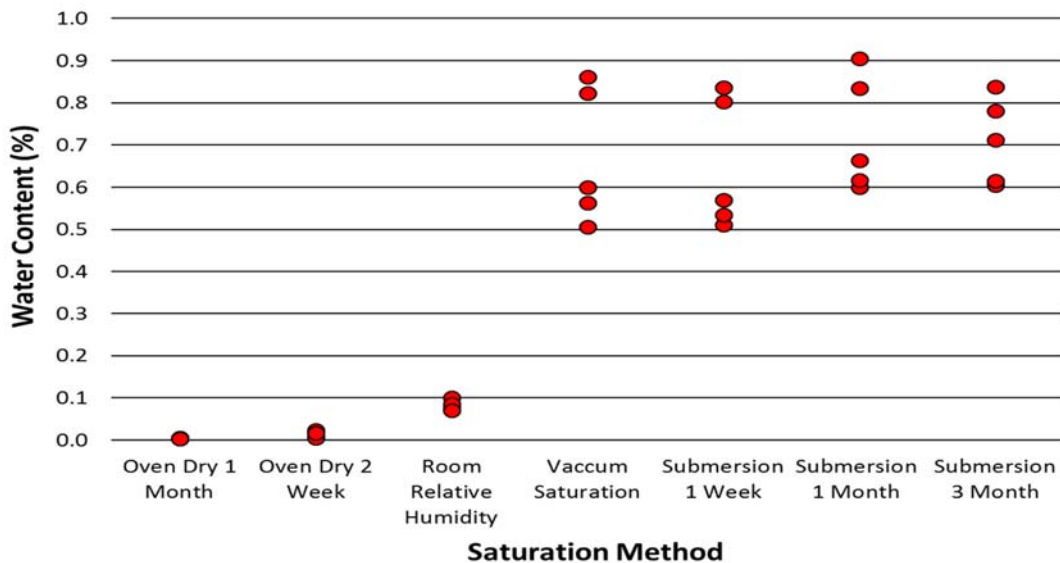


Figure 33: Comparison of water content and saturation method for BTS specimens

Both oven drying methods have decrease the water content to almost zero (with the two week and one month drying resulting in 0.013% and 0.004% average specimen water contents, respectively). The average water content for the RRH specimens is 0.081%. These averages are much lower than those of UCS specimens prepared to the same conditions. Conversely, the water contents of the saturated specimens are higher than those observed for the UCS specimens. In addition to higher water contents, the saturated BTS specimens also have a larger variation in water content in comparison to the UCS specimens. However, the four saturation methods have produced comparable ranges and averages for the water content of BTS specimens. The vacuum and one-week saturation methods resulted in

average water contents of 0.671% and 0.651%, respectively. The one-month saturation specimens resulted in an average water content of 0.724, while the three-month saturation produced an average water content of 0.710%. The variation in water content for saturated BTS specimens is larger than that observed for UCS specimens, but is relatively consistent across all four saturation methods. This increased variability is likely associated with the heterogenous lithology and structure present in the Cobourg limestone. The BTS specimens are more susceptible to this heterogeneity as each specimen is more likely to vary from the next, incorporating different proportions of calcite and clay rich limestone.

7.2.1.2 BTS

The BTS of each specimen has been plotted against water content to investigate the influence of saturation (Figure 34).

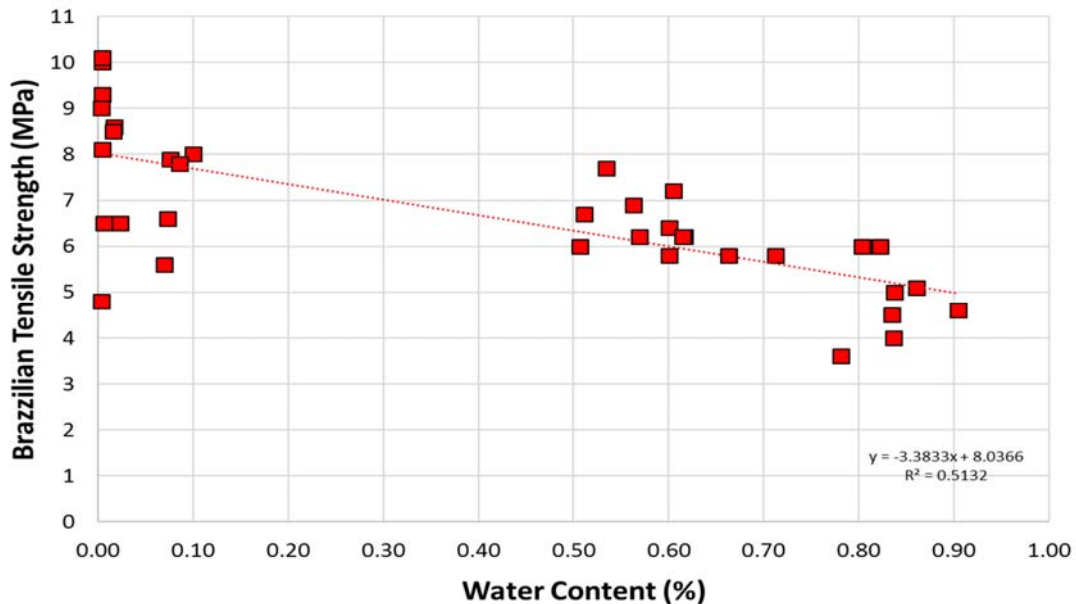


Figure 34: Comparison of BTS with respect to water content for saturation specimens

The data for the saturation specimens shows a significant decreasing trend for BTS with increasing water content. There is a large amount of variability in the BTS results for the oven-dried specimens, specifically the one-month dried specimens which have BTSs ranging from 4.8 to 10.1 MPa. The minimum, maximum, and average BTS for the saturation specimens has been summarized in Table 18.

Table 18: BTS data for saturation specimens

Saturation Condition	BTS (MPa)		
	Min.	Max.	Avg.
Oven Dry 1 Month	4.8	10.1	8.64
Oven Dry 2 Week	6.5	8.6	7.64
Room Relative Humidity	5.6	8.0	7.18
Vacuum Saturation	5.1	6.9	6.08
Submersion 1 Week	4.0	7.7	6.12
Submersion 1 Month	4.5	6.2	5.38
Submersion 3 Month	3.6	7.2	5.56

The average BTSs suggests the same decreasing trend with increased water content and saturation duration. The one and three-month saturated specimens produced the lowest

averages, 5.38 and 5.56 MPa, respectively. The vacuum and one-week saturated specimens also produced similar result. The vacuum saturated specimens had an average of 6.08 MPa, while the one-week saturation specimens had an average of 6.12 MPa.

7.2.2 Scale

The influence of scale on the BTS of Cobourg limestone has been investigated through the testing of Brazilian discs with varying diameter. Specimens have been prepared with diameters of 50 mm (2"), 76 mm (3"), 101 mm (4"), and 126 mm (5"). Each of the specimens has been prepared with a thickness to diameter ratio of 0.5. In total, 17 BTS tests have been conducted to in investigate the influence of scale. The results of this testing have been plotted with respect to specimen diameter in Figure 35.

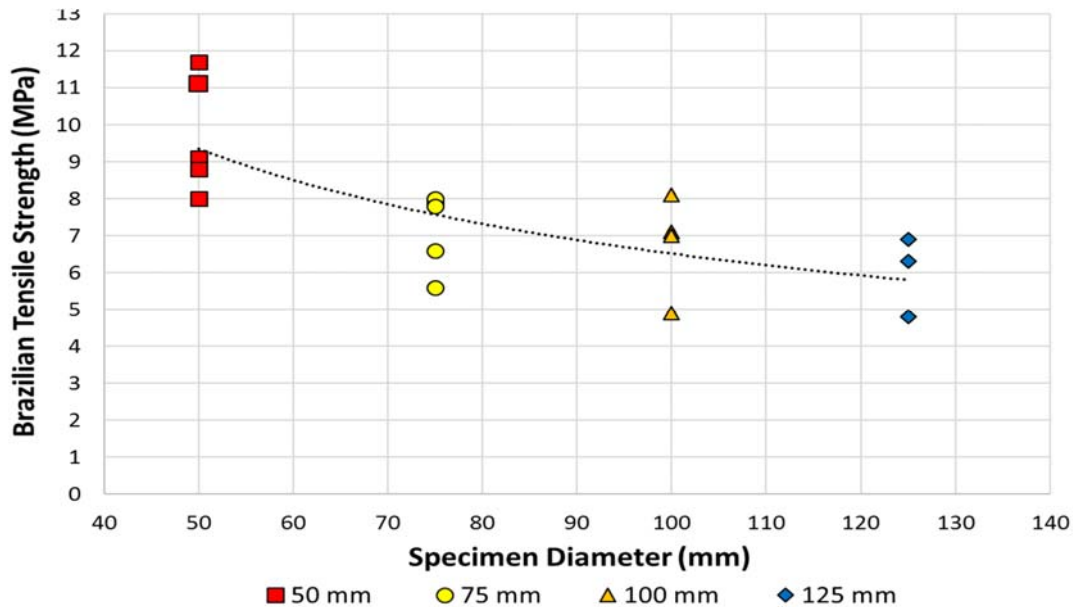


Figure 35: Comparison of BTS with respect to specimen diameter for scale specimens

The scale test results suggest a decreasing trend for BTS with increasing specimen diameter, however, with the trend appearing to plateau as specimen diameter continues to increase. The decrease in average BTS between the 50 and 76 mm is significant, dropping from 9.74 to 7.18 MPa. There is a small decrease between the average BTS of the 76 and 101 mm specimens, with the larger diameter producing an average of 6.78 MPa. The 126 mm specimens produced the lowest average, 6.00 MPa, representing a 38.4% decrease from average 50 mm results. .

Table 19 shows the minimum, maximum, and average BTS.

Table 19: BTS data for scale specimens

Specimen Diameter (mm)	BTS (MPa)		
	Min.	Max.	Avg.
50	8.0	11.7	9.74
76	5.6	8.0	7.18
101	4.9	8.1	6.78
126	4.8	6.9	6.00

8. CONCLUSION

In this study the stress-strain behaviour of Cobourg limestone was investigated using 54 Uniaxial Compressive Strength (UCS) and 47 Brazilian Tensile Strength (BTS) specimens. These specimens were prepared from large blocks collected from St. Mary's Quarry located in Bowmanville, Ontario. The testing of UCS specimens included investigating the effect of saturation, scale, and loading rate on the elastic and strength properties of the rock. The purpose of the BTS testing was to examine the influence of specimen saturation and scale on the tensile strength of the Cobourg limestone.

The effects of saturation on the geomechanical properties of the Cobourg limestone were investigated through the testing of 18 UCS and 30 BTS specimens prepared using six different drying and saturation methods. An additional three UCS and five BTS specimens were included within the saturation data set, representing a seventh saturation condition (76 mm diameter Room Relative Humidity).

The different saturation methods have proven to be more effective for the BTS specimens, drying and saturating the specimens more significantly than for UCS specimens. This behaviour can be attributed to the increased lithological variability presented by the BTS specimens in comparison to the UCS specimens. The UCS specimens are a more homogenous representation of the calcite and clay rich layers of the Cobourg limestone, while the BTS specimens are more likely to be composed of varying portions of these layers.

The longest saturation duration, three-month submersion, did not produce significantly higher water contents in comparison to the other methods. In addition, the three-month saturation duration has the highest likelihood of interaction with the Synthetic Pore Water (SPW) used to saturate the specimens, and may result in some sample deterioration. The lack of increased water content and potential for specimen damage from this saturation method suggests that shorter saturation durations would be adequate for future testing.

Increasing water content in UCS specimens has resulted in increased Poisson's ratio and decreased Young's modulus. The thresholds of CD, UCS, and BTS have shown a significant decreasing trend with increasing water content. CI threshold exhibits a more modest decrease with increasing water content, producing a small range in values that appears to approach a constant value at higher water contents.

Saturation of the clay rich layers of the rock in unconfined conditions is believed to be an important factor influencing the results of this study. The trends observed in this data are likely associated with the localized uptake of SPW into clay rich lenses inherent in the Cobourg limestone.

The influence of specimen scale was studied using 12 UCS and 17 BTS specimens prepared with four different diameters. The changing scale had no significant effect on the Poisson's ratio, CI, CD, or UCS of Cobourg limestone. Examination of the Young's modulus results has shown a consistent increase with specimen diameter, increasing the average modulus by approximately 18% between the 50 and 126 mm specimens. The BTS specimens have shown a consistent decreasing trend throughout all four diameters, with the largest drop in average BTS between the 50 and 76 mm specimens (approximately 26%).

The results of 24 UCS specimens were used to investigate the effect of loading rate on RRH and one-month saturated specimens using four different axial strain rates. In addition, the results of the RRH and one-month saturated specimens used to study the influence of saturation were included in this data set to provide a fifth loading rate (20 min failure time) for additional comparison. The RRH specimen results show a decrease in CD and UCS

threshold with increasing axial strain rate. Young's modulus, Poisson's ratio, and CI threshold remain relatively constant throughout all tested strain rates, suggesting no loading rate effects.

The one-month saturated specimens show the opposite trend of the RRH specimens for CD and UCS. These thresholds increase with increasing axial strain rate, while CI remains constant. Although there appears to be a minor increasing trend in both Young's modulus and Poisson's ratio with increasing axial strain rate, the data at the lower strain rates is quite variable. It is likely that these properties remain relatively constant throughout the different strain rates.

REFERENCES

- Al, T., Xiang, Y., Cave, L. 2010. Measurement of Diffusion Properties by X- Ray Radiography and by Through-Diffusion Techniques Using Iodide and Tritium Tracers: Core Samples from OS-1 and DGR-2. NWMO Technical Report TR-08-27, University of New Brunswick.
- ASTM. 2008a. Designation: D4543-08: Standard Practices for Preparing rock core as cylindrical test specimens and verifying conformance to dimensional and shape tolerances, ASTM International, West Conshohocken, PA.
- ASTM. 2008b. Designation D3967-08: Standard Test Method for Splitting Tensile Strength of Intact Rock Core Specimens. ASTM International, West Conshohocken, PA.
- ASTM. 2010. Designation D2216-10: Standard Test Methods for Laboratory Determination of Water (Moisture) Content of Soil and Rock by Mass, ASTM International, West Conshohocken, PA.
- ASTM. 2014. Designation: D7012-14: Standard Test Methods for Compressive Strength and Elastic Moduli of Intact Rock Core Specimens under Varying States of Stress and Temperatures, ASTM International, West Conshohocken, PA.
- Bieniawski, Z.T. 1967. Mechanism of brittle fracture of rock: Part I – Theory of the fracture process. *International Journal of Rock Mechanics and Mining Sciences*, 4: 395-406.
- Brace, W.F., Paulding, B.W. Jr, Scholz, C. 1966. Dilatancy in the Fracture of Crystalline Rocks. *Journal of Geophysical Research*, 71(16): 3939-3953.
- Diederichs, M.S. 1999. Instability of hard rockmasses: The role of tensile damage and relaxation. PhD Thesis, Department of Civil Engineering, University of Waterloo, Waterloo, Ontario, Canada.
- Diederichs, M.S., Kaiser, P.K., Eberhardt, E. 2004. Damage initiation and propagation in hard rock during tunnelling and the influence of near-face stress rotation. *International Journal of Rock Mechanics and Mining Sciences*, 41: 785-812.
- Dunning, C.P. & Yeskis, D.J. 2007. Lithostratigraphic and Hydrogeological Characteristics of the Ordovician Sinnipee Group in the Vicinity of Waupun, Fond du Lac County, Wisconsin, 1995-96. U.S. Geological Survey, Reston, Virginia.
- Fairhurst, C.E., Hudson, J.A. 1999. International Society for Rock Mechanics, Commission on Testing Methods: Suggested Method for the complete stress-strain curve for intact rock in uniaxial compression. *International Journal of Rock Mechanics and Mining Science*. 36(3): 279-289.
- Ghazvinian, E. 2010. Modelling and testing strategies for brittle fracture simulation in crystalline rock samples. MSc Thesis, Department of Geological Sciences and Geological Engineering, Queen's University, Kingston, Ontario, Canada.
- Ghazvinian, E. 2015. Fracture initiation and propagation in low porosity crystalline rocks: Implications for Excavation Damage Zone (EDZ) mechanics. PhD Thesis, Department of Geological Sciences and Geological Engineering, Queen's University, Kingston, Ontario, Canada.
- Hoek, E. & Brown, E.T. 1980. *Underground excavations in rock*. Institution of Mining and Metallurgy, London, England.
- ISRM. 1979. International Society for Rock Mechanics, Commission on Standardisation of Laboratory and Field Tests: Suggested methods for determining water content, porosity, density, absorption and related properties and swelling and slake-durability index properties. *International Journal of Rock Mechanics and Mining Science*, 16(2): 141-156.
- Lajtai, E.Z., and Lajtai, V.N. 1974. The evolution of brittle fracture in rocks. *Journal of the Geological Society of London*, 130: 1-18.
- Martin, C.D. 1993. The strength of massive Lac du Bonnet granite around underground openings. PhD Thesis, Department of Civil and Geological Engineering, University of Manitoba, Winnipeg, Manitoba, Canada.

Appendix

Appendix 1: Certificate of calibration for the MTS load sensor



MTS Systems Corporation Calibration Laboratory

14000 Technology Drive
Eden Prairie, MN 55344

Certificate of Calibration

For MTS Asset Number: SN291539

Description: PRESSURE TRANSDUCER
Mfr / Model: MTS/660.23A-05
Serial Number: 291539
Certificate #: e3b81c8a2590e64b96ccd5499ec0d7b2
Customer: QUEEN'S UNIVERSITY
Job #: US2.49301

This document applies only to the calibration of the item described above and the specific calibration performed by the MTS Calibration Laboratory. If shown below, the calibration interval has been requested or agreed upon by the customer. When declaring in tolerance or out of tolerance condition(s) the MTS Calibration Laboratory utilizes the Shared Risk Method* as the decision rule. The stability of the UUT over time depends on many factors outside our control. It is the responsibility of those using the item described above to quantify their measurement uncertainty and evaluate the adequacy of their measurement process to demonstrate that measurement traceability is credibly maintained.

The MTS Calibration Laboratory complies with the international standard for calibration laboratories, ISO/IEC 17025 "General Requirements for the Competence of Calibration and Testing Laboratories".

MTS Calibration Laboratory measurement standards, calibration processes, and measurement results are traceable to the International System of Units (SI Unit) through one or more of the following: National Institute of Standards and Technology (NIST), other National Metrology Institutes (NMI's), natural physical constants, consensus standards or by a ratio technique.

CALIBRATION INFORMATION

Received: IN TOLERANCE **Calibration Date:** (mmddyy) 03/07/14 **Temperature:** 72°F
Returned: IN TOLERANCE **Humidity:** 28 %
Calibration Procedure: 1504 **Procedure Revision:** D
Note: NONE

STANDARDS USED FOR CALIBRATION

MTS Asset #	Description	Cal. Date	Cal. Due
19804	PRESSUREMENTS, P3124-3, DW PRESSURE CALIBRATOR	01/31/13	01/30/15
20025	MTS, 494.26, SIGNAL CONDITIONER	05/18/13	05/16/14

Certified by: Yadessa Tikure, Calibration Technician

Printed on: 03/07/2014

Page 1 of 2

If you have questions regarding this Certificate of Calibration please call 952-937-4133. This certificate may not be reproduced, except in full, without written approval from the MTS Calibration Laboratory.
MTS Calibration Form (Rev. 9/10)

*When parameter(s) are certified to be within specified tolerance(s), the measured value(s) shall fall within the appropriate specification limit and the uncertainty of the measured value shall be stated and provided to the customer for evaluation. With written agreement from the customer, other decision rules may be used.

Appendix 2: Certificate of calibration for the MTS axial extensometers



**MTS Systems Corporation
Calibration Laboratory**

14000 Technology Drive
Eden Prairie, MN 55344



Certificate of Calibration

For MTS Asset Number: SN10435642D
Description: EXTENSOMETER
Mfr / Model/Option: MTS/632.11F-90/NONE
Serial Number: 10435642D_10435642E_10435642F
Certificate #: 2e50a09d3c98014abab1332a215dfb2c
Customer: QUEEN'S UNIVERSITY
Job #: US1.51116

This document applies only to the calibration of the item described above and the specific calibration performed by the MTS Calibration Laboratory. If shown below, the calibration interval has been requested or agreed upon by the customer. When declaring in tolerance or out of tolerance condition(s) the MTS Calibration Laboratory utilizes the Shared Risk Method* as the decision rule. The stability of the UUT over time depends on many factors outside our control. It is the responsibility of those using the item described above to quantify their measurement uncertainty and evaluate the adequacy of their measurement process to demonstrate that measurement traceability is credibly maintained.

The MTS Metrology Laboratory has been accredited by the American Association for Laboratory Accreditation (A2LA Certificate Number 1044.01) to perform calibration in electrical, mechanical, dimensional, time/frequency, temperature/humidity, and vibration. The basis for this accreditation is the international standard for calibration laboratories, ISO/IEC 17025 "General Requirements for the Competence of Calibration and Testing Laboratories" and ANSI/NCCL Z540-1.

MTS Calibration Laboratory measurement standards, calibration processes, and measurement results are traceable to the International System of Units (SI Unit) through one or more of the following: National Institute of Standards and Technology (NIST), other National Metrology Institutes (NMI's), natural physical constants, consensus standards or by a ratio technique.

CALIBRATION INFORMATION			
Received:	IN TOLERANCE	Calibration Date:	10-Oct-2014
Returned:	IN TOLERANCE	Temperature:	72°F
		Humidity:	29 %
		Calibration Procedure:	1510
		Procedure Revision:	D
Note:	NONE		

STANDARDS USED FOR CALIBRATION			
MTS Asset #	Description	Cal. Date	Cal. Due
18252	MTS, 650.05-01, EXTENSOMETER CALIBRATOR	19-Jun-2014	19-Dec-2014
20018	MTS, 494.26, SIGNAL CONDITIONER	07-Jun-2014	05-Jun-2015

Certified by: David Reigel, Calibration Technician Printed on: 10-Oct-2014 Page 1 of 2

If you have questions regarding this Certificate of Calibration please call 952-937-4133. This certificate may not be reproduced, except in full, without written approval from the MTS Calibration Laboratory.
MTS Calibration Form (Rev. 9/10)

*When parameter(s) are certified to be within specified tolerance(s), the measured value(s) shall fall within the appropriate specification limit and the uncertainty of the measured value shall be stated and provided to the customer for evaluation. With written agreement from the customer, other decision rules may be used.



Extensometer Calibration Data

Page: 2 of 2 Day/Month/Year
10/Oct/14

Customer		System Number	MTS I.D. Code	
Queen's University		US1.51116.LKM-11	3049-10435642D	
Transducer		Model Number	Option Number(s)	Transducer Sn.
632.11F-90		001	10435642D	10435642E
Excitation Voltage		Calibration Temp / Humidity	Gage Length	Transducer Sn.
10.000 V		72°F / 29%	50.000 mm	10435642F
Conditioner		System Conditioner	Calibration Conditioner	Model Number
		X		494.26
		MTS Asset:20018		

Notes
 ID Module: None Polarity: Inverted
 Gain: 424.47471 DeltaK: 0.9984
 Calibrated using 3in1 cable
 Cable Length: <350FT

Range Full Scale Displacement: ±4.000 mm = ± 10.000 V Nominal

Final calibration. No Linearization correction factors applied.					±4.000 mm = ± 10.000 V Nominal
Delta K	In (+)	In (-)	Out	Shunt Volt. (V) / Shunt Ref. (mm)	Shunt Cal Resistor
Condition			X	-5.275/-2.1101	24.9 K

Displacement						
Micrometer Head Indicated Displacement (millimeters)	Conditioner Output (Volts)	Conditioner Calculated Displacement (millimeters)	Error (% of Reading)	Error (as % of Full Scale Range)	Nominal (% of Full Scale Range)	
-4.0000	-10.0067	-4.0027	0.067	0.067	-100	
-2.8000	-6.9998	-2.7999	-0.003	-0.002	-70	
-1.6000	-3.9975	-1.5990	-0.063	-0.025	-40	
-0.8000	-1.9979	-0.7992	-0.105	-0.021	-20	
-0.4000	-0.9988	-0.3995	-0.120	-0.012	-10	
-0.3200	-0.7990	-0.3196	-0.125	-0.010	-8	
-0.2400	-0.5993	-0.2397	-0.117	-0.007	-6	
-0.1600	-0.3995	-0.1598	-0.125	-0.005	-4	
-0.0800	-0.1997	-0.0799	-0.150	-0.003	-2	
0.0000	0.0000	0.0000	n/a	<0.001	Start at 0	
Tension (-)	0.0000	-0.0013	-0.0005	n/a	-0.013	Return to 0
Compression (+)	0.0000	0.0006	0.0002	n/a	0.006	Return to 0
0.0000	0.0000	0.0000	n/a	<0.001	Start at 0	
0.0800	0.2000	0.0800	<0.001	<0.001	2	
0.1600	0.3999	0.1600	-0.025	-0.001	4	
0.2400	0.6000	0.2400	<0.001	<0.001	6	
0.3200	0.8000	0.3200	<0.001	<0.001	8	
0.4000	1.0002	0.4001	0.020	0.002	10	
0.8000	2.0001	0.8000	0.005	0.001	20	
1.6000	4.0002	1.6001	0.005	0.002	40	
2.8000	7.0000	2.8000	<0.001	<0.001	70	
4.0000	10.0008	4.0003	0.008	0.008	100	

Calibration specification: Greater of: ±1% of reading or ±0.00508 mm.
 Calibration Laboratory displacement measurement expanded uncertainty (U): ±0.2% of reading + 0.00033 mm
 U is calculated using a coverage factor (k) of 2.0, for an estimated confidence probability of 95%.

Performed By: D.Reigel Day/Month/Year
10/Oct/14

Appendix 3: Certificate of calibration for the MTS chain (circumferential) extensometer



**MTS Systems Corporation
Calibration Laboratory**

14000 Technology Drive
Eden Prairie, MN 55344



Amended Certificate of Calibration

For MTS Asset Number: SN10448893C
Description: EXTENSOMETER
Mfr / Model / Option: MTS/632.11F-90/NONE
Serial Number: 10448893C
Original Certificate #: 121d95bb87ce6c4dab74d1f31ee88c99
Amended Certificate #: 10/21/2015 3:52:51PM
Customer: QUEEN'S UNIVERSITY
Job #: US1.51446

This document applies only to the calibration of the item described above and the specific calibration performed by the MTS Calibration Laboratory. If shown below, the calibration interval has been requested or agreed upon by the customer. When declaring in tolerance or out of tolerance condition(s) the MTS Calibration Laboratory utilizes the Shared Risk Method* as the decision rule. The stability of the UUT over time depends on many factors outside our control. It is the responsibility of those using the item described above to quantify their measurement uncertainty and evaluate the adequacy of their measurement process to demonstrate that measurement traceability is credibly maintained.

The MTS Metrology Laboratory has been accredited by the American Association for Laboratory Accreditation (A2LA Certificate Number 1044.01) to perform calibration in electrical, mechanical, dimensional, time/frequency, temperature/humidity, and vibration. The basis for this accreditation is the international standard for calibration laboratories, ISO/IEC 17025 "General Requirements for the Competence of Calibration and Testing Laboratories" and ANSI/NCSL Z540-1.

MTS Calibration Laboratory measurement standards, calibration processes, and measurement results are traceable to the International System of Units (SI Unit) through one or more of the following: National Institute of Standards and Technology (NIST), other National Metrology Institutes (NMI's), natural physical constants, consensus standards or by a ratio technique.

CALIBRATION INFORMATION

Received: IN TOLERANCE	Calibration Date: 10-Oct-2014	Temperature: 72°F
Returned: IN TOLERANCE	Calibration Date: 9-Oct-2015	Humidity: 29 %
	Calibration Procedure: 1510	Procedure Revision: D

Note: AMENDED due to incorrect Gain in original report.

STANDARDS USED FOR CALIBRATION

MTS Asset #	Description	Cal. Date	Cal. Due
18252	MTS, 650.05-01, EXTENSOMETER CALIBRATOR	19-Jun-2014	19-Dec-2014
20018	MTS, 494.26, SIGNAL CONDITIONER	07-Jun-2014	03-Jul-2015

Certified by: David Reigel, Calibration Technician

Printed on: 21-Oct-2015

Page 1 of 2

If you have questions regarding this Certificate of Calibration please call 952-937-4133. This certificate may not be reproduced, except in full, without written approval from the MTS Calibration Laboratory.
MTS Calibration Form (Rev. 9/10)

*When parameter(s) are certified to be within specified tolerance(s), the measured value(s) shall fall within the appropriate specification limit and the uncertainty of the measured value shall be stated and provided to the customer for evaluation. With written agreement from the customer, other decision rules may be used.



Extensometer Calibration Data

Page: 2 of 2 Day/Month/Year
10/Oct/14

Customer		System Number	MTS I.D. Code
Queen's University		US1.51116.LKM-11	3049-10448893C
Transducer		Vendor Serial Number	
Model Number	Option Number(s)	10448893C	
632.11F-90	001		
Excitation Voltage	Calibration Temp / Humidity	Gage Length	Type
10.000 V	72°F / 29%	19.100 mm	Displacement
Conditioner		Model Number	
System Conditioner	Calibration Conditioner	494.26	MTS Asset:20018
	X		
Notes		Cable Length	
ID Module: None Polarity: Normal Gain: 386.4790 DeltaK: 1.0000 Calibrated using ChainKit		<350FT	

Range		Full Scale Displacement
Final calibration. No Linearization correction factors applied.		±4.000 mm = ± 10.000 V Nominal
Delta K	In (+)	In (-)
Condition	Out	x
		7.079/2.8317
		49.9 K

Displacement						
Micrometer Head Indicated Displacement (millimeters)	Conditioner Indicated Output (Volts)	Conditioner Calculated Displacement (millimeters)	Error (% of Reading)	Error (as % of Full Scale Range)	Nominal (% of Full Scale Range)	
-4.0000	-9.9983	-3.9993	-0.017	-0.017	-100	
-2.8000	-6.9991	-2.7996	-0.013	-0.009	-70	
-1.6000	-4.0006	-1.6002	0.015	0.006	-40	
-0.8000	-2.0003	-0.8001	0.015	0.003	-20	
-0.4000	-1.0000	-0.4000	<0.001	<0.001	-10	
-0.3200	-0.7999	-0.3200	-0.012	<0.001	-8	
-0.2400	-0.5997	-0.2399	-0.050	-0.003	-6	
-0.1600	-0.3999	-0.1600	-0.025	-0.001	-4	
-0.0800	-0.2000	-0.0800	<0.001	<0.001	-2	
0.0000	0.0000	0.0000	n/a	<0.001	Start at 0	
Compression (-)	0.0000	-0.0011	-0.0004	n/a	-0.011	Return to 0
Tension (+)	0.0000	0.0004	0.0002	n/a	0.004	Return to 0
	0.0000	0.0000	0.0000	n/a	<0.001	Start at 0
	0.0800	0.2000	0.0800	<0.001	<0.001	2
	0.1600	0.3999	0.1600	-0.025	-0.001	4
	0.2400	0.6001	0.2400	0.017	<0.001	6
	0.3200	0.8002	0.3201	0.025	0.002	8
	0.4000	1.0003	0.4001	0.030	0.003	10
	0.8000	2.0015	0.8006	0.075	0.015	20
	1.6000	4.0034	1.6014	0.085	0.034	40
	2.8000	7.0096	2.8038	0.137	0.096	70
	4.0000	10.0200	4.0080	0.200	0.200	100

Calibration specification: Greater of: ±1% of reading or ±0.00508 mm.
 Calibration Laboratory displacement measurement expanded uncertainty (U): ±0.2% of reading + 0.00033 mm
 U is calculated using a coverage factor (k) of 2.0, for an estimated confidence probability of 95%.

Performed By:	D.Reigel	Day/Month/Year	10/Oct/14
----------------------	----------	----------------	-----------

Appendix 4: Specification sheet for HBM strain gauges.



Dehnungsmessstreifen
Strain gages
Jauges d'extensométrie

Bestellnummer
Order No.
No. de référence

Typ
Type
Type

Stückzahl
Contents
Quantité

Temperaturkoeffizient
des k-Faktors
Temperature coefficient
of gage factor
Coefficient de température
du facteur k

Folienlos
Lot
Lot de la feuille

Herstellungslas
Batch
Lot de fabrication

K-LY4-1-09-120-3-3

10/120 LY41-3L-3M

10

93 ± 10 [10⁻⁶ / °C]
(-10°C ... +45°C)

A406/12

812050813

Widerstand
Resistance
Résistance

k-Faktor
Gage factor
Facteur k

Querempfindlichkeit
Transverse sensitivity
Sensibilité transverse

2,06 ± 0,35 %

2,06 ± 1,0 %

0,2 %

Temperaturkompensation: Angepasst für
Temperature compensation: Compensated for
Compensation de température: Compensation pour

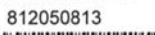
Ferritischen Stahl mit
steel with
acier avec

$\alpha = 10,8 [10^{-6} / ^\circ\text{C}]$

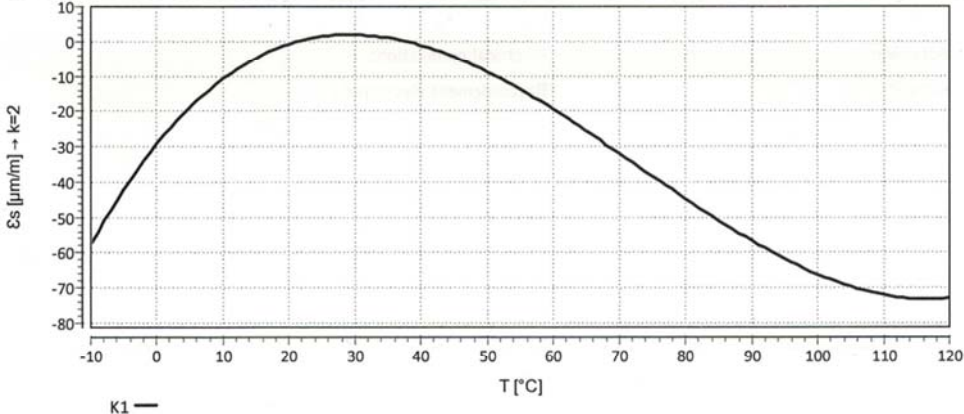












K1 —

$\epsilon_s (T) = -16,16 + 1,67 \cdot T - 4,96E-02 \cdot T^2 + 2,27E-04 \cdot T^3 + 0,650 \cdot (T-20) [\mu\text{m}/\text{m}] \pm 0,30 [\mu\text{m}/\text{m}/^\circ\text{C}]$

Alle technischen Daten nach OIML IR 62, bei Beachtung der abweichenden Toleranzangaben, auch nach VDI/VDE 2635. Geben Sie bei Rückfragen bitte Bestellnummer und Herstellungs-Los an.

All specifications in accordance with OIML IR 62, also compliant with VDI/VDE 2635 if deviating tolerances are observed. In case of further inquiries please indicate order no. and batch number.

Toutes caractéristiques techniques selon OIML IR 62 et VDI/VDE 2635 pour les indications différentes de tolérance. Pour toutes questions, indiquer le no. de référence ainsi que le lot de fabrication.

Réponse en température des jauges d'extensométrie appliquées sur des matériaux dont les coefficients de dilatation thermique α sont indiqués au verso. Mesurée au d'une variation continue de la température.

Courbe 1: Jauges avec câble en PVC.
T = température en °C

Temperaturgang der Dehnungsmessstreifen bei Applikationen mit unseitig angegebenen Wärmeausdehnungskoeffizienten α . Gemessen bei kontinuierlicher Temperaturänderung.

Kennlinie 1: DMS mit PVC Kabel.
T = Temperatur in °C

The **temperature response** refers to strain gages bonded to materials with the coefficient of thermal expansion α given overleaf. Values are measured with continuous temperature variation.

Curve 1: Strain gages with PVC cable.
T = temperature in °C

Kopfdaten / Header / Titre



Appendix 5: UCS data summary for all tests.

	#	Specimen #	Description	Water Content (%)	Test Date	Axial Displacement Rate (mm/min)	Radial Displacement Rate (mm/min)	UCS (Mpa)	Young's Modulus (GPa)		Poisson's Ratio		
									E 35	E50	v 35	v50	
									Scale effect				Loading rate effect (75 mm)
Scale effect	RRH, 200 µε/min												
	1	C1-6-1-U	50mm	0.13	10-Mar-16	0.01	0.00825	135.01	38.177	36.663	0.1933	0.2128	
	2	C1-8-1-U	specimens	0.12	10-Mar-16	0.01	0.00825	135.01	37.798	37.327	0.1965	0.2204	
	3	C1-13-1-U		0.12	10-Mar-16	0.01	0.00825	123.79	35.894	35.015	0.1796	0.2048	
	4	C1-4-1-U	75mm	0.32	11-Oct-15	0.01	0.0125	114.28	40.497	38.706	0.2069	0.2570	
	5	C1-9-1-U	specimens	0.26	11-Oct-15	0.01	0.0125	127.88	38.929	37.939	0.2069	0.2358	
	6	C1-12-1-U		0.18	29-Oct-15	0.01	0.0125	106.80	40.195	38.395	0.2385	0.2752	
	7	B1-1-1-U	100mm	0.18	29-Nov-16	0.01	0.0165	112.61	37.842	36.634	0.2197	0.2427	
	8	B2-1-1-U	specimens	0.21	29-Nov-16	0.01	0.0165	111.31	42.889	46.159	0.3918	0.7685	
	9	B2-2-1-U		0.16	29-Nov-16	0.01	0.0165	128.38	41.592	40.013	0.231	0.2521	
	10	C1-1-1-U	125mm	0.12	24-Mar-16	0.01	0.021	133.58	45.841	44.193	0.2224	0.2457	
	11	C1-5-1-U2	specimens	0.12	25-Mar-16	0.01	0.021	118.86	46.12	45.39	0.1827	0.2242	
12	C1-10-1-U		0.12	25-Mar-16	0.01	0.021	124.10	44.93	43.135	0.2227	0.2467		
Loading rate effect (75 mm)	Room RH												
	13	A1-3-1-U2	specimens	0.28	15-Oct-15	0.03	0.0375	111.95	43.656	42.909	0.219	0.2281	
	14	C2-2-1-U	are failed in 6 min	0.31	15-Oct-15	0.03	0.0375	123.48	41.616	39.877	0.2257	0.2388	
	15	A1-5-1-U		0.07	29-Oct-15	0.03	0.0375	123.05	43.233	41.634	0.2306	0.2968	
	16	A1-4-1-U	specimens	0.27	17-Oct-15	0.0003	0.000375	122.50	34.54	33.632	0.2098	0.2324	
	17	C2-3-1-U	are failed in 600 min	0.10	22-Jan-16	0.0003	0.000375	129.34	38.322	37.288	0.2269	0.2557	
	18	A1-9-1-U		0.21	7-Nov-15	0.0003	0.000375	133.86	38.226	37.219	0.2239	0.2424	
	19	A1-7-1-U	specimens	0.27	17-Oct-15	0.1	0.125	128.30	42.226	40.642	0.2448	0.2629	
	20	C2-2-2-U	are failed in 2 min	0.29	17-Oct-15	0.1	0.125	87.80	35.397	33.797	0.2147	0.2452	
	21	A1-11-1-U		0.24	22-Oct-15	0.1	0.125	128.34	40.866	39.341	0.2127	0.2358	
	22	A1-8-1-U	specimens	0.27	20-Oct-15	0.003	0.00375	125.52	35.694	34.679	0.2183	0.2407	
	23	C2-8-1-U	are failed in 60 min	0.22	22-Oct-15	0.003	0.00375	135.02	38.553	37.551	0.146	0.2011	
	24	A1-12-1-U		0.19	7-Nov-15	0.003	0.00375	132.77	41.414	28.015	0.2266	0.1683	
	25	A1-3-2-U	specimens	0.66	19-Nov-15	0.03	0.0375	100.29	32.375	30.006	0.2408	0.3051	
	26	C2-11-1-U	are failed in 6 min	0.71	19-Nov-15	0.03	0.0375	90.62	31.975	32.662	0.2999	0.325	
	27	C2-12-2-U		0.65	19-Jan-16	0.03	0.0375	81.23	25.687	25.348	0.2413	0.3296	
	28	A1-4-2-U	specimens	0.51	19-Nov-15	0.0003	0.000375	84.28	28.689	28.554	0.1523	0.2197	
	29	C2-14-1-U	are failed in 600 min	0.55	21-Nov-15	0.0003	0.000375	99.97	28.838	27.915	0.2732	0.3657	
	30	A1-15-1-U		0.56	28-Nov-15	0.0003	0.000375	75.11	20.726	17.772	0.11	0.1198	
	31	A1-7-2-U	specimens	0.66	19-Nov-15	0.1	0.125	103.15	33.073	30.609	0.1969	0.2621	
	32	C2-15-1-U	are failed in 2 min	0.75	21-Nov-15	0.1	0.125	84.20	33.29	31.607	0.2402	0.3027	
	33	A1-16-1-U		0.64	21-Nov-15	0.1	0.125	98.65	31.806	30.036	0.2709	0.3571	
	34	A1-8-2-U	specimens	0.55	25-Nov-15	0.003	0.00375	84.47	33.098	31.975	0.2339	0.2992	
	35	C2-16-1-U	are failed in 60 min	0.72	25-Nov-15	0.003	0.00375	69.31	34.638	37.21	0.232	0.4698	
	36	C2-4-1-U		0.64	28-Nov-15	0.003	0.00375	78.03	26.019	25.582	0.185	0.2491	
	Saturation Effect (75 mm)	200 µε/min											
		37	A2-6-1-U	Oven-dry (1 month)	0.06	12-Nov-15	0.01	0.0125	151.76	45.022	42.94	0.2375	0.2578
		38	A2-12-1-U		0.05	12-Nov-15	0.01	0.0125	140.97	37.533	36.382	0.2194	0.2623
		39	A2-15-2-U		0.05	12-Nov-15	0.01	0.0125	139.11	39.079	37.313	0.2011	0.2212
		40	A2-5-1-U	Oven-dry (2 weeks)	0.07	27-Oct-15	0.01	0.0125	123.05	43.233	41.634	0.2306	0.2968
		41	A2-11-1-U		0.11	27-Oct-15	0.01	0.0125	138.69	43.528	41.044	0.1635	0.1953
		42	A2-15-1-U		0.08	29-Oct-15	0.01	0.0125	99.30	36.753	37.048	0.2028	0.276
		43	C1-4-1-U	75mm	0.32	11-Oct-15	0.01	0.0125	114.28	40.497	38.706	0.2069	0.257
		44	C1-9-1-U	specimens	0.26	11-Oct-15	0.01	0.0125	127.88	38.929	37.939	0.2069	0.2358
		45	C1-12-1-U		0.18	29-Oct-15	0.01	0.0125	106.80	40.195	38.395	0.2385	0.2752
		46	A2-2-1-U	Submerged (1 week)	0.59	3-Nov-15	0.01	0.0125	95.37	35.283	33.787	0.2658	0.3099
47		A2-8-1-U		0.62	3-Nov-15	0.01	0.0125	91.19	36.125	34.302	0.2355	0.2716	
48		A2-13-1-U		0.62	5-Nov-15	0.01	0.0125	103.59	37.845	35.704	0.2241	0.2547	
49		A2-1-1-U	Pressurized (1 week)	0.59	26-Nov-15	0.01	0.0125	99.33	34.965	32.532	0.2249	0.2667	
50		A2-7-1-U		0.61	3-Dec-15	0.01	0.0125	103.43	34.823	32.927	0.2412	0.2792	
51		A2-12-2-U		0.62	3-Dec-15	0.01	0.0125	89.25	33.53	32.402	0.2255	0.2625	
52		A2-3-1-U	Submerged (1 month)	0.62	1-Dec-15	0.01	0.0125	77.21	32.946	32.21	0.2764	0.3721	
53		A2-9-1-U		0.57	1-Dec-15	0.01	0.0125	86.67	33.118	31.562	0.184	0.2581	
54		A2-14-1-U		0.64	3-Dec-15	0.01	0.0125	86.42	25.534	26.115	0.2303	0.3464	
55		A2-4-1-U	Submerged (3 months)	0.66	19-Jan-16	0.01	0.0125	83.99	30.625	28.593	0.2246	0.2875	
56	A2-10-1-U		0.58	19-Jan-16	0.01	0.0125	96.18	32.489	30.308	0.2862	0.384		
57	A2-14-2-U		0.71	19-Jan-16	0.01	0.0125	84.98	23.093	22.702	0.2416	0.3398		

Specimen #	Crack Initiation (CI) Threshold					Critical Damage (CD) Threshold			Acoustic Emission			
	Direct Circumferential Strain (MPa)	Crack Volumetric Strain CI_L (MPa)	Crack Volumetric Strain CI_U (MPa)	Inverse Tangent Lateral Stiffness (MPa)	Instantaneous Poisson's Ratio (MPa)	Direct Axial Strain (MPa)	Direct Volumetric Strain (MPa)	IYM (MPa)	Acoustic Emission CI_L (MPa)	Acoustic Emission CI_M (MPa)	Acoustic Emission CI_U (MPa)	Acoustic Emission CD (MPa)
C1-6-1-U	48	47	57	57	57	95	na	125	na	53	na	119
C1-8-1-U	55	47	53	49.5	50	105	na	118	38	48	58	108
C1-13-1-U	51	46	55	na	na	92	115.0	94	32	52	72	107
C1-4-1-U	48	36	47	47	47	90	112	106	37	51	65	102
C1-9-1-U	47	45	49	na	na	98	na	120	45	57	68	100
C1-12-1-U	49	38	51	46	50	98	86.0	85	41	52	63	92
B1-1-1-U	46	43	46	61	N/A	82	82	82	42	N/A	61	76
B2-1-1-U	43	N/A	N/A	39	39	100	N/A	N/A	39	N/A	53	105
B2-2-1-U	46	48	57	66.5	56	98	N/A	120	N/A	66	N/A	114
C1-1-1-U	53	44	55	48	55	97	na	119	na	53	na	107
C1-5-1-U2	55	na	62	na	58	93	na	107	na	50	na	103
C1-10-1-U	49	45	47	39	na	96	112.0	108	36	45	54	117
A1-3-1-U2	52	na	na	58	55	82	na	105	38	47	51	83
C2-2-1-U	54	54	61	54	44	84	na	110	36	50	60	97
A1-5-1-U	48	43	58	na	55	88	na	106	31	50	69	109
A1-4-1-U	48	39	50	48	48	85	na	100	33	48	62	105
C2-3-1-U	54	46	54	41	40	102	106	100	30	56	78	107.8
A1-9-1-U	62	43	54	na	na	95	na	112	38	45	61	124
A1-7-1-U	58	na	54	46	48	98	na	101	36	na	55	80
C2-4-2-U	46	34	42	39	39	64	76	68	na	44	na	67
A1-11-1-U	52	45	56	51	53	87	na	105	47	na	56	100
A1-8-1-U	55	44	55	58	57	80	na	101	31	51	71	100
C2-8-1-U	52	52	52	na	na	100	na	120	38	na	61	118
A1-12-1-U	48	na	na	na	na	64	na	na	42	49	64	85
A1-3-2-U	39	38	39	39	37	55	94	80	31	38	48	98
C2-11-1-U	55	33	38	54	53	75	80	65	na	61	na	75
C2-12-2-U	na	28	33	33	36	62	62.0	66	37	na	52	72
A1-4-2-U	38	33	35	34	32	66	64	64	na	31	na	65
C2-14-1-U	37	36	38	36	34	74	75	73	33	39	55	87
A1-15-1-U	43	na	na	42	40	64	na	62	25	37	52	64
A1-7-2-U	38	37	44	44	44	64	92	na	37	na	52	65
C2-15-1-U	36	30	35	29	33	62	73	70	26	35	46	82
A1-16-1-U	38	36	40	31	34	70	75.0	na	34	na	50	74
A1-8-2-U	39	33	35	48	48	65	65	na	38	na	57	78
C2-16-1-U	27	25	32	32	26	na	38	na	23	31	41	41
C2-4-1-U	43	29	na	43	na	66	73.0	73	na	40	na	72
A2-6-1-U	62	na	59	50	50	116	132	132	na	56	na	129
A2-12-1-U	52	51	51	51	50	112	121	112	40	54.5	69	105
A2-15-2-U	41	35	39	na	na	78	90.0	92	41	53	65	104
A2-5-1-U	56	46	57	56	55	98	110	111	42	58	62	111
A2-11-1-U	41	48	48	na	na	88	na	135	39	53.5	68	125
A2-15-1-U	42	38	38	58	58	77	90	na	41	53	65	84
C1-4-1-U	48	36	47	47	47	90	112	106	37	44.5	52	90
C1-9-1-U	47	45	49	na	na	98	na	120	45	58.5	72	100
C1-12-1-U	49	38	51	46	50	98	86	85	42	53	64	92
A2-2-1-U	44	36	na	46	na	70	84	74	39	44.5	50	83
A2-8-1-U	43	31	40	46	na	68	na	74	32	51	54	88
A2-13-1-U	48	35	51	50	42	59	94	89	40	46.5	53	93
A2-1-1-U	45	34	42	48	46	67	na	80	39	45	51	90
A2-7-1-U	46	37	42	49	50	62	na	82	36	56	64	82
A2-12-2-U	42	34	39	38	na	63	80	77	32	46	51	66
A2-3-1-U	39	29	33	36	38	52	55	67	34	44.5	55	63
A2-9-1-U	39	30	33	37	na	57	na	74	na	46	na	64
A2-14-1-U	40	31	36	42	43	68	55	61	na	37	na	61
A2-4-1-U	38	30	37	36	36	55	na	74	32	34.5	37	63
A2-10-1-U	38	36	42	40	40	66	70	86	na	39	na	92
A2-14-2-U	39	34	na	44	na	62	71	72	na	34	na	76

Appendix 6: Brazilian Tensile Strength (BTS) data summary for all tests.

		#	Specimen #	Brazilian ID	Description	Brazilian Strength (MPa)	Average Brazilian Strength (MPa)	Water Content (%)
Scale effect	Room RH	1	C1-4-1-U	c1-4-bot-1	75mm specimens	6.6	7.2	0.07
		2		c1-4-bot-2		7.9		0.08
		3	C1-2-1-U	c1-2-top		8.0		0.10
		4	C1-12-1-U	c1-12-top		7.8		0.09
		5		c1-12-bot		5.6		0.07
		6	C1-6-1-U	c1-6-1		9.1		0.10
		7		c1-6-2	11.1	0.07		
		8	C1-8-1-U	c1-8-1	11.7	9.7	0.08	
		9		c1-8-2	8.0	0.08		
		10	C1-13-1-U	c1-13-1	8.8	0.07		
		11	B1-1-1-U	B1-1-Top-1	4.9	100mm Specimens	6.8	0.16
		12	B2-1-1-U	B2-1-Top-1	8.1			0.18
		13		B2-1-Top-2	7.1			0.14
14	B2-2-1-U	B2-2-Top-1	7.0	0.18				
15	C1-1-U	c1-1	6.9	125mm specimens	6.0	0.31		
16	C1-5-U	c1-5	4.8			0.33		
17	C1-10-U	c1-10	6.3			0.31		
Saturation effect		18	A2-1-1-U	a2-1-top	Pressurized (1 week)	6.4	6.1	0.60
		19		a2-1-bot-1		6.0		0.82
		20	A2-7-1-U	a2-7-top		6.0		0.51
		21		a2-7-bot		5.1		0.86
		22	A2-4-1-U	a2-4-top-3		6.9		0.56
		23	A2-2-1-U	a2-2-top		6.7		Submerged (1 week)
		24		a2-2-bot	6.0	0.80		
		25		A2-8-1-U	a2-8-top-1	7.7	0.53	
		26	A2-8-1-U	a2-8-bot-1	4.0	0.84		
		27		A2-13-1-U	a2-13-top	6.2	0.57	
		28	A2-3-1-U	a2-3-top	5.8	Submerged (1 month)	5.4	
		29		a2-3-bot	4.6			0.90
		30	A2-9-1-U	a2-9-top	6.2			0.62
		31		a2-9-bot	4.5			0.83
		32	A2-10-1-U	a2-10-top-2	5.8			0.66
		33	A2-4-1-U	a2-4-top-1	7.2			Submerged (3 months)
		34		a2-4-top-2	5.8	0.71		
		35	A2-10-1-U	a2-10-top-1	6.2	0.62		
		36		a2-10-bot-1	5.0	0.84		
		37		a2-10-bot-2	3.6	0.78		
		38	A2-5-1-U	a2-5-top	6.5	Oven-dry (2 weeks)	7.6	
		39		a2-5-bot	6.5			0.02
		40	A2-11-1-U	a2-11-top-1	8.1			0.00
41	a2-11-bot-2	8.6		0.02				
42	a2-11-top-2	8.5		0.02				
43	A2-6-1-U	a2-6-top	10.0	Oven-dry (1 month)	8.6			0.00
44		a2-6-bot	4.8			0.00		
45	A2-8-1-U	a2-8-top-2	10.1			0.00		
46		a2-8-bot-2	9.3			0.00		
47	A2-1-1-U	a2-1-bot-2	9.0			0.00		